~~Calibration of basal melt on past ice discharge lowers projections of Antarctica's~~ Antarctic dynamics contribution to future sea level ~~contribution~~ constrained by ice discharge observations

Eveline C. van der Linden[1], Dewi Le Bars[1], Erwin Lambert[1], and Sybren Drijfhout[1,2]

[1]Royal Netherlands Meteorological Institute, Utrechtseweg 297, 3731 GA, De Bilt, The Netherlands
[2]Institute for Marine and Atmospheric Research Utrecht, Department of Physics, Utrecht University, Princetonplein 5, 3584 CC, Utrecht, The Netherlands

Correspondence: Eveline C. van der Linden (linden@knmi.nl)

Abstract. Antarctic mass loss is the largest contributor to uncertainties in sea level projections on centennial timescales. In this study we aim to constrain future projections of the contribution of Antarctic dynamics by using ice discharge observations. The contribution of Antarctica's ice discharge ~~to future sea level changes~~ is computed with ocean thermal forcing from 14 earth system models (ESMs) and linear response functions (RFs) from 16 ice sheet models for three ~~greenhouse gas emission~~ 5 ~~scenarios. Different than in~~ shared socio-economic pathway (SSP) scenarios. New compared to previous studies, basal melt ~~was calibrated on observed Antarctic ice discharge rather than on basal melt itself with an iterative approach. For each model combination, a linear and quadratic melt dependency were calibrated both regionally (in five Antarctic sectors) and at the continental scale. Projections using all model combinations show that the variation in basal melt computation methods~~ sensitivities to ocean temperature changes were calibrated on four decades of observed ice discharge changes rather than using 10 observation-based basal melt sensitivities. The results show that even with calibration the acceleration during the observational period is underestimated, indicating missing physics. Also the relative contribution of the Amundsen region is underestimated. The Amundsen contribution and sea level acceleration improved by using an Amundsen-specific calibration (rather than Antarctic-wide), quadratic basal melt parameterisation (rather than linear) and thermal forcing near the ice shelf base (rather than the deepest layer above the continental shelf). Although calibration improved historical performance, calibration alone 15 did not reduce the uncertainty in the projections. Uncertainties associated with ESMs and RFs affect the projected sea level contribution more than the ~~scenario variations (SSP1-2.6 to SSP5-8.5). After calibration, a high number of model pairs still underestimated ice discharge in hindcasts over 1979-2017. Therefore top 10% best-performing model combinations were selected for each method. A comparison between these model selections shows that the quadratic melt parameterisation with Antarctic-wide calibration performs best in reproducing past ice discharge. We conclude that calibration of basal melt on past~~ 20 ~~ice discharge combined with model selection makes projections of Antarctic ice discharge (more) consistent with observations over the past four decades. Moreover, calibration of basal melt on past ice discharge results in lower basal melt sensitivities and thus lower~~ SSP scenario variations and methodological choices in the calibration and basal melt computation method. Despite the different method applied, the resulting projections of Antarctica's sea level contribution ~~than estimates of~~ are in line with

previous multi-model studies .(ISMIP6, LARMIP-2). However, our results suggest that constraining their basal melt relation with ice discharge observations in the Amundsen region will lead to higher future estimates.

1 Introduction

Sea level rise poses an increasing threat to densely populated coasts and deltas worldwide (Hinkel et al., 2014). Even if the 1.5 degree target of the Paris Agreement is met, global mean sea level will rise several meters in the longer term (Clark et al., 2016; Fox-Kemper et al., 2021). At present, a global acceleration of sea level rise is visible in satellite measurements and the sea level is already rising more than twice as fast as the average rate over the twentieth century (Nerem et al., 2018; Dangendorf et al., 2019).

Mass loss from land ice (ice sheets and glaciers) is currently accelerating and is now (over the period 2006–2018) the largest contributor to the global mean sea level rise (Fox-Kemper et al., 2021). Antarctic ice sheet (AIS) mass loss has tripled over the last decade (Shepherd et al., 2018), which can be mainly attributed to increased ice discharge in the Amundsen Sea (Rignot et al., 2019). Models and geological data indicate that the Antarctic ice sheet AIS will cause most of the sea level rise in the long term over thousands of years (Bamber et al., 2019). Moreover, melt of Antarctic land ice is the largest contributor to uncertainties on centennial timescales (Palmer et al., 2020; van de Wal et al., 2019). The degree of acceleration of future sea level changes is mainly determined by dynamic processes on the Antarctic ice sheetAIS. The underlying processes are 1) increased melt from below by warmer ocean water (basal melt) and 2) increased calving (iceberg formation) triggered by basal melt and/or surface melt (Rignot and Jacobs, 2002; Pritchard et al., 2012; Liu et al., 2015; van den Broeke, 2005). It is important to gain a better understanding of the many uncertainties about the Antarctic contribution to sea level rise that exist and to reduce these uncertainties when possible to support adaptation planning (Haasnoot et al., 2020). Uncertainties associated with the Antarctic contribution to sea level rise even appear to be increasing. Using similar methodologies to each other, the estimated Antarctic contribution in Levermann et al. (2020) shows increased uncertainty compared to its previous study (Levermann et al., 2014) and expert judgment assessments of Bamber et al. (2019) give higher uncertainties than before (Bamber and Aspinall, 2013). To address this issue our study aims to gain more insight in the Antarctic contribution to and uncertainties in future sea level changes and provides directions for reducing these uncertainties.

Future projections of Antarctic mass loss are often based on modelling studies. Most earth system models (ESMs) do not have interactive ice sheet modules, because ice sheet models are particularly sensitive to small changes in the climate and often assume unrealistic geometries if they have to be balanced with the data from ESMs. This means that changes in the mass loss of an ice sheet are not (properly) predicted by ESMs and that ice sheets in coupled ice sheet-ESMs show undesirable and unrealistic trends. The proper functioning of ice sheet models in an earth system model is a worldwide effort for which no effective solution can be expected in the short term. Therefore, , in which ice sheet models are often used as a standalone unit and balanced with observations. In this setup the forcing of ice sheet models forcing is provided by ESMs. earth system models (ESMs). Over the last decade, ice sheet modelling has advanced from single model studies to model intercomparison projects (MIPs). In these projects, earth system modelling and ice sheet modelling are combined to make pro-

jections of land ice. The Ice Sheet ~~MIP (ISMIP~~Model Intercomparison Project for CMIP6 (ISMIP6) (Nowicki et al., 2016) and Linear Antarctic Response ~~MIP (LARMIP~~Model Intercomparison Project (LARMIP-2) (Levermann et al., 2020) are currently used as ~~a~~ one basis for projections of the Antarctic land ice evolution (Fox-Kemper et al., 2021). ISMIP6 (Seroussi et al., 2020)

60 provides process-based projections of the sea level contribution of the ~~Antarctic ice sheet~~ AIS based on a variety of ice sheet models that are forced by atmosphere and ocean output from CMIP5 ESMs. ISMIP6 made a selection of six ESMs based on two main criteria. The first criterion is based on their performance in reproducing the mean state of the current climate (atmosphere and ocean) near Antarctica, but did not include trends. The second criterion ensures that the ESM selection includes a diversity of warming rates over the 21st century so that the uncertainty-range in projections is captured (Barthel et al., 2020;

65 Nowicki et al., 2020). One risk of ~~the second criterion~~ this selection process is that models with a relatively bad performance over the historical period in terms of trends could have been chosen. ~~Bias metrics for the selection included criteria on the mean state of the ocean and atmosphere, but did not include trends.~~ In ISMIP6 basal melt ~~was chosen to depend quadratically on thermal forcing (Favier et al., 2019) and~~ is calibrated on basal melt observations ~~in two regions (mean Antarctic ice sheet and the Pine IslandGlacier grounding line)~~ with two options for calibration: the mean AIS and Pine Island's grounding line

70 (Jourdain et al., 2020). LARMIP-2 focuses on ice sheet mass loss due to ice shelf basal melt (Levermann et al., 2014, 2020). In that study, the temperature melt-relation is parameterised with a linear dependency on thermal forcing. ISMIP6 and LARMIP-2 have thirteen ice sheet models in common and are primarily based on the CMIP5 ~~models~~ ESMs and scenarios (RCPs) as forcing. Edwards et al. (2021) estimated probability distributions for projections under the ~~new~~ SSP scenarios based on CMIP6 ESMs, by using statistical emulation of the ISMIP6 ice sheet models.

75 Our study follows LARMIP-2 to account for the sensitivity of ice sheet models to climate change by using linear response functions (RF) of ice sheet models. The LARMIP-2 RFs were obtained by prescribing for five regions an immediate change in basal melt of the ice ~~sheet~~ shelves and simulating the resulting increase in ice sheet discharge with the ice sheet model. In this way a relationship between basal melt and mass loss is obtained for each region~~. Another~~: the linear response function. Additionally, a relationship between thermal forcing and basal melt is used to compute basal melt from ocean temperatures: the

80 basal melt parameterisation. These relationships, together with a time-dependent warming derived from ESMs, then lead to a time-dependent mass loss of the ice sheet. This method was applied by Levermann et al. (2014, 2020) to a number of ice sheet models. In those studies, CMIP5 models were used to diagnose the relationship between global surface air temperature (GSAT) and ocean temperature changes around Antarctica, and GSAT was used as a driver of the method. The advantage of using GSAT over ocean temperature changes as driver is that also uncertainties in GSAT changes were included in the uncertainty estimate.

85 Furthermore, GSAT is easier to derive, but it does not account for (future changes in) Southern Ocean dynamics. It could be expected that a regional metric has a better relation with forcing underneath ice shelves. Therefore, the current study improves this step by using subsurface ocean temperature as driver (Lambert et al., 2021). In addition to the linear melt ~~dependency~~ parameterisation as in the Levermann et al. (2020) study, a more advanced quadratic basal melt parameterisation is applied since observation-based evidence suggests a nonlinear relationship between melting and ocean temperature (Jenkins et al.,

90 2018).

The basal melt parameterisations are calibrated on observation-based estimates of ice discharge changes (Rignot et al., 2019), rather than on basal melt as is done in ISMIP6. One advantage of using ice discharge measurements is that they capture the entire ice sheet through satellite measurements of ice height and velocity and therefore are better constrained than basal melt estimates which are not measured for the full ice sheet and for the full time period that we use for calibration. Moreover, when using basal melt for calibration, basal melt observations are required long before the actual ice discharge acceleration takes place due to the delayed response of ice discharge to basal melt. The advantage of this new approach is that ice discharge acceleration during the historical period is directly derived from observations, thereby constraining the basal melt even before the observational period. As calibration target the mass loss estimates of Rignot et al. (2019) were chosen over Shepherd et al. (2018) for two reasons. The first reason is that Rignot et al. does not include surface mass balance processes which makes the data directly comparable with our resultsthe linear response functions that only represent the contribution of Antarctic dynamics. The second reason is that the Rignot et al. record starts earlier which allows us to look into mass loss acceleration during a longer period. Two different calibrations calibration methods are applied: at the regional and a regional calibration on the Amundsen sector and one at the continental scale. By applying the same melt relation to the past and the future, we ensure that the physics is consistent with four decades of observed mass loss. Here, the assumption is that no new processes are taking place. Using different warming scenarios and RFs for a variety of models, we arrive at an a new estimate of the future mass loss of Antarctica that is consistent with observed mass loss over the past four decadesand the Amundsen sector that is constrained by observed ice discharge.

2 Methodology

In this study the contribution of changes in Antarctica's ice discharge to sea level changes is computed with state-of-the-art ESMs from Coupled Model Intercomparison Project Phase 6 (CMIP6; Eyring et al. 2016) and linear response functions from the Linear Antarctic Response MIP (LARMIP-2; Levermann et al. 2020) ice sheet models.

Flow diagram of procedure. Observational constraints are indicated in orange, main computations of the Levermann et al. method in green (including model experiments by the modelling groups), calibration methods in yellow, bias-adjustment in grey and (intermediate) output data in blue. The continuous lines represent direct pathways while the dashed lines refer to iterative processes or optional choices during calibration.

The basic procedure of this study follows that of Levermann et al. (2020) with a number of modifications as explained below and illustrated in Fig. 1.

2.1 Ocean forcing

Earth system models from CMIP6 are used as a basis for the computations, guaranteeing implementation of state-of-the-art models in the analysis and projections. Ocean temperatures are directly taken from the CMIP6 models, The ocean forcing consists of annual mean simulated subsurface ocean temperatures which are obtained from ESM output instead of estimating them from scaling coefficients and global mean air temperature. For the representation of basal melt our method employs a
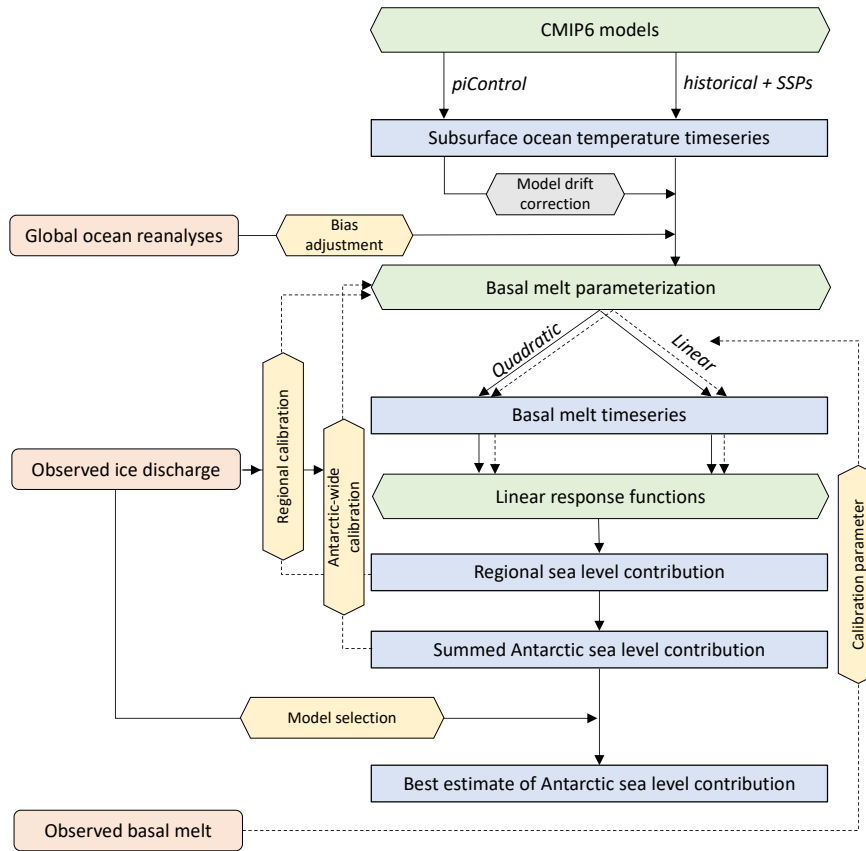
Figure 1. Flow diagram of procedure. Observational constraints are indicated in orange, main computations of the Levermann et al. method in green (including model experiments by the modelling groups), calibration methods in yellow, bias-adjustment in grey and (intermediate) output data in blue. The continuous lines represent direct pathways while the dashed lines refer to iterative processes or optional choices during calibration.

linear as well as a quadratic melt relation with thermal forcing (TF), i.e. the difference between the in situ temperature of sea water (T_o) and the in situ freezing-melting point temperature (T_f):

125    $TF = T_o - T_f.$

Finally, the parameterisations are calibrated on regional or Antarctic-wide observed ice discharge from Rignot et al. (2019). This calibration step is a key difference with the Levermann et al. studies.

2.2   **Ocean forcing**

Table 1. CMIP6 ~~models~~ ESMs that have been evaluated. For each region the subsurface ocean temperature bias (in K) compared to the GREP reanalysis is indicated over the period 1993-2018, including years 2015-2018 for the SSP2-4.5 scenario. The 'drift correction' column indicates whether the piControl experiment was used for model drift correction~~or~~. The bottom rows show the ~~historical experiment~~mean and standard deviation (σ) of the ESM biases and the mean ocean temperature (in °C) and standard deviation of the GREP reanalysis product.

CMIP6 ~~model~~ ESM	EAIS	Weddell	Amundsen	Ross	Peninsula	Drift correction
ACCESS-CM2	-0.33	-0.11	-1.05	-1.26	0.09	~~historical~~
CAMS-CSM1-0	0.24	-0.05	0.22	-0.94	0.39	piControl
CAS-ESM2-0	1.43	0.79	0.20	-0.18	2.18	~~historical~~
CMCC-ESM2	0.31	-0.23	0.51	-0.10	0.58	piControl
CanESM5	-0.55	-0.43	-0.07	-0.80	-0.21	piControl
EC-Earth3	0.06	-0.57	1.17	0.71	-0.33	~~historical~~
EC-Earth3-Veg	-0.10	-0.58	0.84	0.44	-0.34	piControl
GFDL-ESM4	0.05	-0.38	0.45	-1.00	0.20	piControl
INM-CM4-8	-0.37	0.32	-0.66	-0.17	0.19	piControl
INM-CM5-0	-0.74	-0.24	-1.16	-1.11	-0.16	piControl
MIROC6	0.81	0.55	1.58	1.40	0.29	~~historical~~
MPI-ESM1-2-LR	-0.31	0.03	0.08	-0.59	-0.41	piControl
MRI-ESM2-0	-0.12	-0.10	-0.12	-0.31	0.32	~~historical~~
NorESM2-MM	-0.92	-0.45	-0.71	-0.84	-0.74	piControl
Bias Mean	-0.04	-0.10	0.09	-0.34	0.15	-
~~Std~~ Bias σ	0.59	0.40	0.78	0.74	0.67	-
GREP Mean	0.53	-0.79	1.37	-0.18	-0.24	
GREP σ	0.23	0.21	0.24	0.53	0.21	

~~The ocean forcing consists of annual mean simulated subsurface ocean temperatures by CMIP6 ESMs. The ocean temperatures~~
GSAT as in LARMIP-2 (Lambert et al., 2021). The ocean temperatures are taken from the historical experiment (1850-2014) and the Shared Socioeconomic ~~Pathways~~ Pathway (SSP) ~~scenarios~~ SSP1-2.6, SSP2-4.5 and SSP5-8.5 (2015-2100). Only models that have data available at the Earth System Grid Federation (ESGF) data server for the historical experiment and all three SSP scenarios (at the time of study) are considered. In addition, models should provide data for the full period (1850-2100) without any data gaps since the computation of the delayed ice sheet response to basal melt requires a continuous time series. Table 1 summarises which models have been taken into account.

Ocean temperatures are averaged over five oceanic sectors: the East ~~Antarctic Ice Sheet~~ AIS (EAIS), Ross, Amundsen, Weddell and Peninsula sector (Fig. 2), and averaged vertically over a range of 100 m, centered around the depth of the ice shelf
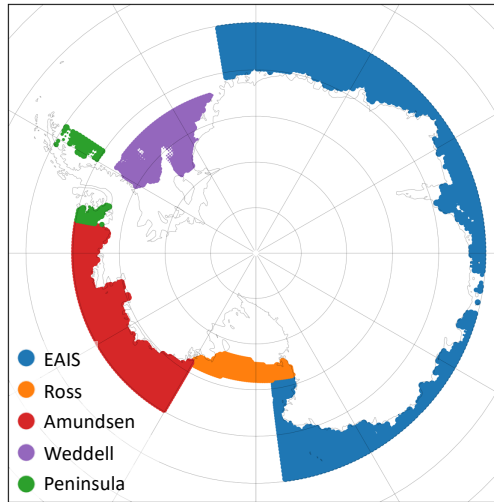
Figure 2. Ocean sector definition.

Table 2. Mean ice shelf depth (in m) for the five sectors in Fig. 2.

Sector	Depth (m)
EAIS	369
Weddell	420
Amundsen	305
Ross	312
Peninsula	420

base (Table 2). In addition, temperatures in an ocean layer around the depth of the continental shelf near the ice shelf front (800-1000 m) were used to assess the impact of thermal forcing depth on the projections (Table 3)(Sect. 3.3.2). Different from

140 Levermann et al. (2020), the Peninsula sector is defined as a separate ocean sector rather than using the same ocean sector coordinates as the Amundsen sector.

The ocean temperature time series are corrected for model drift by removing the long term trend diagnosed by the linear trend in the pre-industral control (piControl) experiment (Fig. 3). For models that did not provide suitable data for the piControl experiment, the model drift is ~~estimated from the historical experiment with a variable detrending period starting in 1850 and~~

145 ~~ending between 1900 and 1950. The smallest absolute trend within this period is considered model drift and removed from the time series. In this way we assure that (multi-)decadal variability has minimal influence on the trend magnitude . For the quadratic melt parameterisaton, the resulting~~ not removed. Although the ocean temperature bias has no clear relation
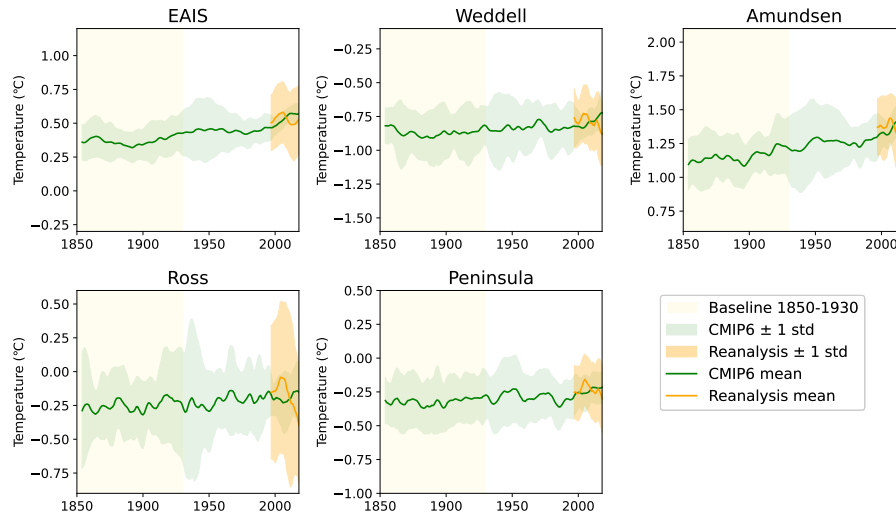
Figure 3. Annual mean subsurface ocean temperature time series ~~smoothed by a five-year running average filter for the~~ averaged over all ESMs (green), model drift- and bias-adjusted~~(green) CMIP6 multi-model mean~~, and the GREP ensemble mean (orange). ~~For CMIP6 models,~~ Both are smoothed by a five-year running average filter. The temperature is derived from a 100-m thick layer centered around the mean depth of the ice shelf base as specified in Table 2. The historical experiment (1850-2014) is combined with SSP2-4.5 (2015-2018) for this visualisation. Note that the tick distances of the vertical axis are the same for all regions, but the ranges are different.

with projected temperature trends in ESMs (Little and Urban, 2016), it affects the magnitude of basal melt in the quadratic parameterisation. Therefore, before computing the basal melt the time mean ocean temperatures are bias-adjusted with global

150 ocean reanalyses called the Global Reanalysis Ensemble Product (GREP). GREP can be obtained from the Copernicus Marine Server at 1 degree horizontal resolution over the period during which altimetry data observations are available (1993-2018). It is constructed by postprocessing of four reanalyses: GLORYS2V4 from Mercator Ocean (France), ORAS5 from ECMWF, FOAM/GloSea5 from Met Office (UK), and C-GLORS05 from CMCC (Italy). ~~Although the ocean temperature bias has no clear relation with projected temperature trends in ESMs (Little and Urban, 2016), it affects the magnitude of basal melt in the~~

155 ~~quadratic parameterisation. Therefore, before computing the basal melt the ocean temperatures are bias-corrected.~~ It should be noted, however, that the reanalysis data may also be biased due to a paucity of assimilated data and the absence of ice shelves in the physical ocean models.

Averaged over all CMIP6 ~~models~~ ESMs the subsurface temperature ~~of the CMIP6 multi-model mean~~ is cold-biased for the EAIS, Weddell and Ross sectors over the 1993-2018 period. For the Amundsen and Peninsula sectors the mean simulated

160 temperature is warm-biased (Table 1). For all regions, the sign of the bias differs between individual models. The ~~ensemble mean bias~~ ocean temperature time series of the individual models are corrected by the ensemble mean of the reanalysis products over the 1993-2018 time period ~~is removed from the modelled ocean temperatures~~ over the entire historical and future period to obtain the bias-adjusted ocean temperatures (Fig. 3).

Table 3. ~~Abbreviations for~~ Overview of basal melt ~~parameterisation~~ computation and calibration methods applied in this study. Two different depths were used for the thermal forcing: centered around the mean depth of the ice shelf base and the layer at 800-1000 m depth. Also, two different basal melt parameterisation methods were employed: linear and quadratic. Each parameterisation has been calibrated Antarctic wide and regionally ~~. Unbounded means that γ has zero as lower limit and no upper limit for at least 95% of the ESM-RF combinations. Bounded means that the Levermann et al. (2020) bounds are applied~~ on the ~~linear parameterisation (both upper~~ Amundsen region. Finally, median basal melt sensitivities used in LARMIP-2 and ~~lower bounds)~~ ISMIP6 have been applied.

~~Abbreviation~~ Thermal forcing depth	Parameterisation relation	~~Calibration bounds Calibration region~~ Basal melt sensitivity
~~QUR~~ Ice shelf base	Quadratic	~~Unbounded Regional~~ Amundsen calibration
~~QUA~~ 800-1000 m	~~Quadratic Unbounded Antarctic LUR~~ Linear	~~Unbounded Regional~~ Antarctic-wide calibration
~~LUA~~	~~Linear~~	~~Unbounded Antarctic~~ ISMIP6 AntMean Median
~~LBR~~	~~Linear~~	~~Bounded Regional~~ LARMIP-2 Median
~~LBA Linear Bounded Antarctic~~ height		

2.2 Basal melt parameterisation

165 ~~Warming of ocean water above the freezing point temperature~~ When the water temperature underneath ice shelves in ice shelf cavities ~~induces~~ reaches the freezing-melting point temperature it will induce basal melt of the corresponding ice shelves. CMIP6 ~~models~~ ESMs, however, typically do not represent ice shelf cavities and the related thermal and dynamical properties. Coastal ocean temperatures should therefore be translated into these cavities. This can be done by using a parameterisation that relates the far-field (coastal) ocean temperature to basal melt. Most of the simple basal melt parameterisations assume a relation

170 with thermal forcing~~,~~, i.e. the difference between the in situ temperature of sea water (T_o) and the in situ freezing-melting point temperature (T_f):

$$TF = T_o - T_f. \tag{1}$$

Our method employs a linear and quadratic melt relation with thermal forcing (Table 3). The quadratic relation was suggested to outperform a linear relation (Favier et al., 2019), but we will apply both so that we can compare our results with the linear

175 relation used in Levermann et al. (2020). The linear relation is defined as:

$$m = \gamma_l \left(\frac{\rho_{sw} c_{po}}{\rho_i L_i} \right) TF, \tag{2}$$

where m is the basal melt and γ_l is the linear calibration parameter. It assumes a constant heat exchange, independent on the local stratification and circulation. The quadratic relation is defined as:

$$m = \gamma_q \left(\frac{\rho_{sw} c_{po}}{\rho_i L_i} \right)^2 TF|TF|. \tag{3}$$

180 where ~~m is the basal melt and γ is~~ the ~~calibration parameter~~ quadratic calibration parameter is γ_q. The basal melt sensitivity is defined as $\gamma_l \left(\frac{\rho_{sw} c_{po}}{\rho_i L_i} \right)$ for the linear relation and $\gamma_q \left(\frac{\rho_{sw} c_{po}}{\rho_i L_i} \right)^2$ for the quadratic relation. The quadratic relation assumes

Table 4. Physical constants.

parameter	symbol	value	unit
ice density	ρ_i	917	kg m^{-3}
sea water density	ρ_{sw}	1028	kg m^{-3}
specific heat capacity of ocean mixed layer	c_{po}	3947	J kg^{-1} K^{-1}
latent heat of fusion of ice	L_i	3.34×10^5	J kg^{-1}
heat exchange velocity	γ	calibrated	m s^{-1}
liquidus slope	λ_1	-0.0575	°C PSU^{-1}
liquidus intercept	λ_2	0.0832	°C
liquidus pressure coefficient	λ_3	7.59×10^{-4}	°C m^{-1}

that the heat exchange scales with the buoyancy-driven cavity circulation and that this scales linearly with the large-scale temperature gradient. The values of the physical constants ρ_{sw}, c_{po}, ρ_i and L_i are given in Table 4. The freezing-melting point temperature T_f underneath ice shelves is computed from the ocean salinity S_o and the depth of the ice shelf base z_b:

185
$$T_f = \lambda_1 S_o + \lambda_2 + \lambda_3 z_b. \tag{4}$$

~~See Table 4 for the values of the physical constants.~~ Favier et al. take T_o and T_f either as local or ~~nonlocal values, where nonlocal is~~ as the product of local and ~~nonlocal (averaged~~ the average over the entire ice draft of a given sector~~) thermal forcing~~. In the current study, a purely nonlocal forcing is applied, similar to DeConto and Pollard (2016) and Levermann et al. (2020). The values of T_o are computed as averages over the five (far-field) oceanic sectors, around the depth of the ice shelf base

190 (see Table 2) ~~. Since most~~ or a deeper layer (800-1000 m depth). Since CMIP6 ~~models~~ ESMs typically do not resolve cavities, the far-field ocean temperature is taken. The underlying assumption is that the ocean temperature remains constant while it is advected into the cavity. ~~Also note that the ocean sectors are somewhat wider than the continental shelf, consistent with Levermann et al. (2020). The advantage of a wider region is that it allows for more assimilated observations in the reanalysis product that is used for the bias adjustment of ocean temperature (the continental shelf region is only sparsely sampled).~~

195 ~~Furthermore, the resolution of most CMIP6 models is not high enough to resolve the ocean circulation on the continental shelf, including the Antarctic Slope Current (Thompson et al., 2018). The~~ The computation of T_f is based on a constant salinity value for each oceanic sector, which is computed from the far-field salinity climatology of the reanalysis data. The resulting values of T_f are approximately -1.6 °C in each sector.

Note that the melt is positive if the ocean temperature exceeds the freezing-melting point temperature and negative (i.e.

200 water is refreezing) otherwise. ~~The change in basal melt anomaly is~~ In the current study, basal melt anomalies are used to compute the sea level contribution. The basal melt anomalies are defined as the difference in basal melt between time t and the baseline time period, 1850-1930. This period was chosen since it is long enough to reduce the impact of natural variability on the baseline but short enough so that it doesn't include the trends due to anthropogenic forcing.

~~Basal melt anomalies in linear parameterisations do not depend on the mean temperature, only on the anomaly. In contrast,~~
~~basal melt computed from the quadratic parameterisation depend on the mean temperature as well. As a consequence, biases~~
~~in ocean temperature will influence the estimated magnitude of basal melt changes. Ocean temperatures were therefore~~
~~bias-adjusted with the ocean reanalysis data.~~ The basal melt parameterisation can be calibrated with the heat exchange velocity
γ. It should be noted that ~~γ has~~ γ_l and γ_q have a different order of magnitude in the linear and quadratic parameterisation~~and is~~, respectively, and are not directly comparable.

2.3 Sea level contribution and calibration

Linear response functions (RFs) from LARMIP-2 will be used to compute the cumulative sea level contribution ΔS (in meters)
due to a change in basal melt Δm for each of the five sectors (Fig. 2):

$$\Delta S(t) = \int_0^t d\tau \, \Delta m(\tau) \cdot RF(t - \tau). \tag{5}$$

The sum of the five regional sea level contributions gives the total Antarctic sea level contribution.

LARMIP-2 provides RFs of 16 ice sheet models. Combined with the 14 ESMs (Table 1), this results in 224 ESM-RF
combinations for the projections. ~~The resulting sea level contributions are calibrated on observation-based ice discharge. For~~
~~each individual sector and the total Antarctic, we have derived the~~ For each ESM-RF pair, the basal melt parameterisation is
calibrated on observed ice discharge from Rignot et al. (2019)~~data. Then the~~. The root-mean-square error (RMSE) between
the observed and modelled cumulative changes in ice discharge for each year, weighted equally, over the period 1979-2017 for
each ESM-RF ~~combination~~ pair is determined over a wide range of γ values ~~.~~ for Eq. (2) and Eq. (3). The RMSE is computed
over the full time series to constrain models on the cumulative sea level change as well as the acceleration. ~~For all calibrations,~~
~~γ should be equal or greater than zero, since negative values would imply that temperatures above the melting point lead to~~
~~ice growth, which is deemed not physically possible.~~ The γ value giving the lowest RMSE for each ESM-RF pair provides the
calibrated ~~γ (Fig. 5).~~
~~The linear~~ basal melt sensitivity. Note that this calibration step is a key difference with the Levermann et al. studies. Levermann et al. (202
does not calibrate the basal melt parameterisation ~~has been calibrated in two ways: with bounded and unbounded γ values~~ on
ice discharge, but uses melt sensitivities derived from observations.

The calibration is applied regionally on the Amundsen region and Antarctic-wide (Table 3)~~. For the 'unbounded' calibrations,~~
~~the upper bound of the~~, resulting in two basal melt sensitivities for each ESM-RF pair for a given parameterisation. Figure 5
shows the basal melt sensitivities corresponding with the calibrated γ ~~range~~ values for the linear and quadratic basal melt
parameterisation and for the two calibration regions. For the Antarctic-wide calibration, the same γ value is applied to
each region. The smallest RMSE between the summed discharge over all regions in observations and models determines
the calibrated γ value. For the Amundsen calibration, the calibrated γ value is determined by the ~~requirement that at least 95%~~
~~of all ESM-RF combinations should have the best fit within the~~ best fit between the modelled response and observations over
only the Amundsen region. The resulting γ ~~range; they have no upper bound. This means that for at most 5% of the ESM-RF~~

pairs there is an upper bound. This resulted in a values are then applied to the other four regions to obtain the Antarctic summed response.

In addition, to assess the impact of our calibration method on the sea level projections, a single calibration parameter (γrange of 0.0-6.0 m yr^{-1} for the quadratic parameterisation and 0.0-0.1 m yr^{-1} for the linear parameterisation. In order to compare our results to Levermann et al. (2020), we also applied a bounded calibration . For the bounded calibration, the basal melt sensitivity (i.e. $\gamma \left(\frac{\rho_{sw} c_{po}}{\rho_i L_f} \right)$) should be in the empirically based range determined by Levermann et al. (2020): 7-16 m yr^{-1} K^{-1}. The bounded calibration is only applied to the linear parameterisation.

The calibration is applied regionally and Antarctic-wide) derived from observed basal melt has been applied to all ESM-RF pairs (Fig. 1). This calibration parameter is derived from the median basal melt sensitivity that was used in LARMIP-2 for the linear parameterisation and ISMIP6 for the quadratic parameterisation (Table 3). For each ESM-RF pair, the γ parameter with the best fit (lowest RMSE) is selected for each of the five sectors in an iterative approach

For all basal melt computation and calibration methods, the Amundsen contribution and the total contribution of the AIS are analysed. The RMSE between observed and modelled ice discharge for these two regions was used to assess the impact of model selection on projections of the Antarctic dynamics contribution to sea level (Fig. 1). For the regional calibration the summed Antarctic response is the sum of the regionally calibrated contributions with five basin-specific γ values. In addition, the calibration is performed with the same γ value in each region, resulting in Antarctic-wide calibrated γ values.

3 Results

3.1 Basal melt computation and calibration

Basal melt is computed from subsurface ocean temperature time series(Fig. 1). . The temperature time series over the historical period are shown in Figures 3and 4 for Figure 3. Figure 4 shows the thermal forcing for part of the historical and future period , respectively(1950-2100). Over the 21st century, all regions show a median warming increase in thermal forcing but the magnitude varies between individual regions and becomes scenario dependent around year 2050 (Fig. 4). 2050.

The basal melt parameterisations are calibrated by fitting the sea level response of each ESM-RF pair on the Rignot ice discharge time series changes in observed ice discharge over the full 1979-2017 period (Rignot et al., 2019). This exercise shows that the median γ parameter basal melt sensitivity value resulting in the lowest RMSE varies between individual regions differs between the Antarctic-wide calibration and calibration on the Amundsen region (Fig. 5). For the Ross and Weddell regions, a relatively low γ gives a better fit with Rignot data, while for the Amundsen and Peninsula regions a higher γ improves the calibration. The EAIS and Amundsen region a higher median basal melt sensitivity than for the Antarctic-summed response improves the fit. The Antarctic-wide calibration give intermediate γ values. The relative magnitudes of the γ values are includes regions with a small or negative past contribution to sea level, resulting in a lower basal melt sensitivity. The relatively high magnitude of the median basal melt sensitivity of the Amundsen region is consistent with the higher sensitivity to ocean warming of the respective regions as described in Dinniman et al. (2016). For regions with a non-zero contribution The contribution of ice discharge to sea level over the observational period , the percentage of greater-than-zero calibrated γ values
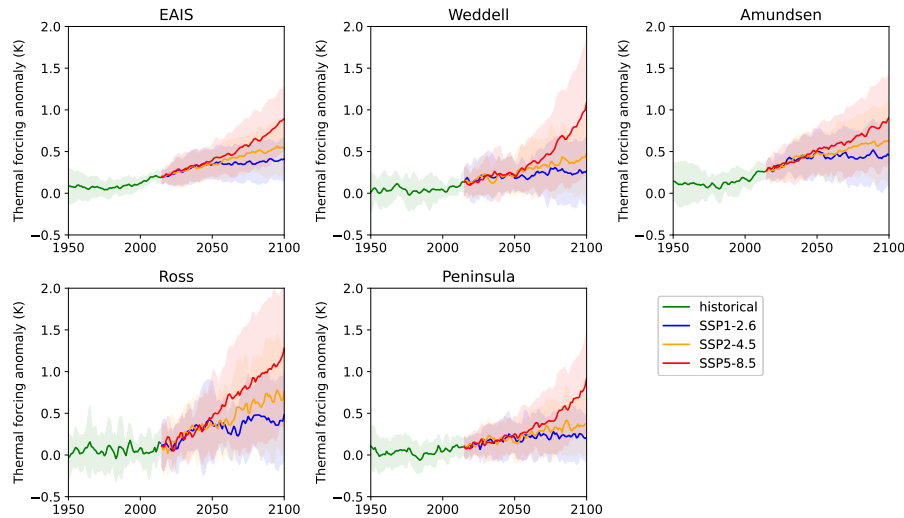
Figure 4. ~~Projections of annual mean subsurface ocean temperature~~ Thermal forcing anomalies for SSP1-2.6, SSP2-4.5 and SSP5-8.5 including all evaluated CMIP6 ~~models~~ ESMs (Table 1) from 1950 to 2100 relative to the baseline period 1850-1930. The shaded regions indicate ~~one associated~~ the intermodel ~~standard deviation. Note that~~ spread (17th to 83rd percentiles) in ocean subsurface temperature between the ~~tick distances of the vertical axis are the same for all regions, but the ranges are different~~ESMs.

~~indicates the percentage of~~ is positive and (at least partly) attributable to ocean warming for both the Amundsen region and the
270 total AIS. Therefore, for each ESM-RF ~~pairs that could be calibrated. For each calibration region, the percentage of~~ pair the calibration parameter, and thus the basal melt sensitivity, should be positive for both Antarctica and the Amundsen region. If the best fit (lowest RMSE) is associated with a negative basal melt sensitivity, this means that the ESM-RF combination could not be calibrated. Between 83% and 90% of all ESM-RF ~~pairs with greater-than-zero calibrated~~γ ~~values (> 0 m yr^{-1}) are therefore indicated~~ could be calibrated, dependent on the parameterisation type and calibration region, as indicated on top of
275 the boxes in Fig. 5. These percentages show that for ~~most calibration regions~~the Antarctic-wide calibration region, the quadratic parameterisation has a higher percentage of positive values than the linear parameterisation. The boxplots only represent the ESM-RF pairs with positive ~~γ values as indicated by the percentages on top. These percentages show that for the Weddell, Ross and Peninsula sectors less than half of the~~ basal melt sensitivities. These calibrated ESM-RF pairs ~~have greater-than-zero γ values. The calibrated γ values~~ are used in the hindcasts and projections of ~~Antarctic~~ changes in ice discharge.

280   For the linear parameterisation, we made a comparison between our ~~positive γ values (calibrated on ice discharge) and the γ~~ calibrated basal melt sensitivities and the values used in LARMIP-2 (Levermann et al., 2020) (green shading in Fig. 5~~, calibrated on basal melt~~). This comparison shows that our Antarctic-wide calibration results in a median ~~γ~~basal melt sensitivity just below the lower bound of the ~~Levermann et al. γ~~LARMIP-2 interval. Regional calibration on the Amundsen sector results in a median basal melt sensitivity above the LARMIP-2 range. Furthermore, the spread in the calibrated basal melt sensitivites
285 is much larger than the spread in the observation-based range. ~~The same applies to the EAIS sector . For the Amundsen and~~
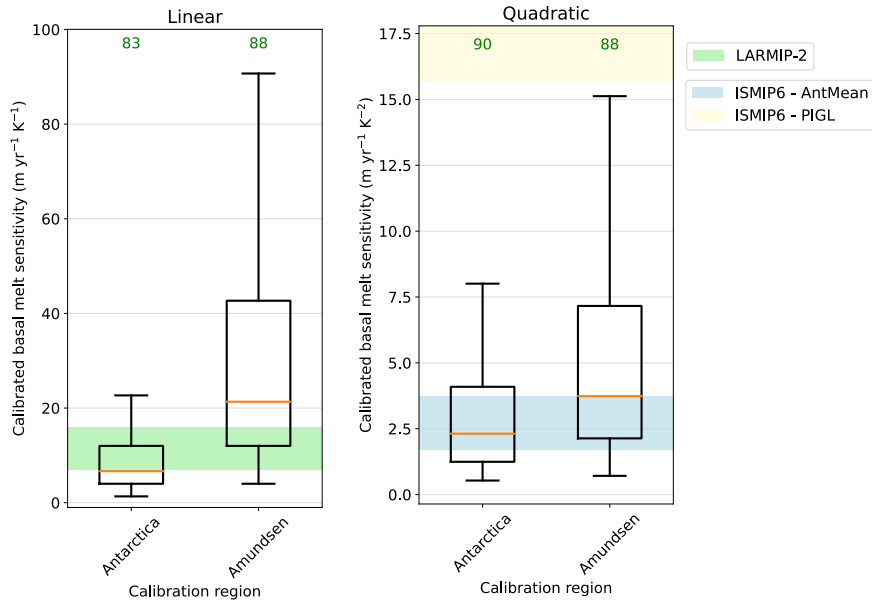
Figure 5. Box-and-whisker plots of basal melt sensitivity values corresponding with the calibrated γ values of ESM-RF pairs. Only the sensitivities of calibrated γ values greater than zero are shown in the plot. The percentage of ESM-RF pairs with positive γ values is indicated by the green values on top of the boxes for each region. The horizontal orange line indicates the median value, boxes indicate the 25-75 percentile range and whiskers the 5-95 percentile range. Values beyond this range are not shown. The shaded regions indicate basal melt sensitivity ranges that are used in other studies. The green shading represents the basal melt sensitivity range of 7-16 m yr^{-1} K^{-1} used in Levermann et al. (2020). The blue and yellow shading indicate the 5-95% range of the basal melt sensitivities corresponding with the γ values used for the nonlocal quadratic parameterisation in ISMIP6 (Jourdain et al., 2020) for both the Antarctic mean (AntMean) and Pine Island's grounding line (PIGL) calibration option, respectively. For PIGL the 95% bound is 84 m yr^{-1} K^{-2}, which is outside the scale of the vertical axis.

~~Peninsula sectors, regional calibration results in γ values at the high end or above the Levermann et al. γ range , while the values for the Ross and Weddell Sea are lower~~ESM-RF pairs with a calibrated basal melt sensitivity above the observation-based range (more than half of the model pairs for the Amundsen calibration) would underestimate historical ice discharge if a random melt sensitivity within the LARMIP-2 range would have been used. Vice versa, ESM-RF pairs with a calibrated sensitivity below the LARMIP-2 range (about half of the model pairs for the Antarctic-wide calibration) would overestimate historical ice discharge if a random melt sensitivity from within the LARMIP-2 range would have been used.

For the quadratic parameterisation, a similar comparison was made with the ~~γ values~~ basal melt sensitivities applied in ISMIP6 (Jourdain et al., 2020). Also for the quadratic paramerisation, ~~our~~ the median Antarctic-wide calibrated ~~γ (calibrated on four decades of observed ice discharge)~~ basal melt sensitivity sits at the lower end of the ~~γ~~ range of the Antarctic mean ~~calibration~~ (AntMean) calibration option (blue shading in Fig. 5~~, calibrated on basal melt)~~) applied in ISMIP6. The ~~median~~

Table 5. Sensitivity of calibration parameter of the quadratic parameterisation to thermal forcing. Values indicate median basal melt sensitivity for calibrated γ values based on three types of thermal forcing. For comparison the median value of the AntMean calibration that is used in ISMIP6 is shown. The first type is the thermal forcing as shown in Fig. 3, which is based on the bias-adjusted ocean subsurface temperature timeseries of the ESMs near the ice shelf base. The second type is based on the same ocean temperature timeseries raised with one standard deviation (1σ) that expresses the spread between the ocean reanalysis products (GREP σ in Table 1). The third type is the thermal forcing at 800-1000 m depth.

Thermal forcing	Antarctic-wide [m yr^{-1} K^{-2}]	Amundsen [m yr^{-1} K^{-2}]	ISMIP6 Antmean
Ice shelf base	2.3	3.7	2.6
Ice shelf base + 1σ	1.8	3.4	-
800-1000 m	1.2	5.5	-

~~EAIS, Ross and Weddell sectors are (just) below the Antarctic mean ISMIP6 range, whereas the~~ Amundsen calibration results in a ~~calibrated median γ at the high~~ median basal melt sensitivity at the top end of the Antarctic mean range ~~and the Peninsula calibration gives a median γ just above the Antarctic mean range~~. In ISMIP6, also a calibration on ~~the Pine IslandGlacier~~ Pine Island's grounding line basal melt was applied as an option (yellow shading in Fig. 5), which is the highest observed basal melt of the ~~Antarctic ice sheet~~AIS. Only some ~~of the~~ calibrations of ESM-RF pairs outside the 95th percentile range resulted in γ values ~~in the Pine Island Glacier~~ within the PIGL range. However, it should be remarked that the ISMIP6 ~~Pine Island Glacier calibration goes together with~~ PIGL calibration also includes negative ocean temperature corrections all around Antarctica that counter-balance the effects of the large γ values ~~.~~ (Jourdain et al., 2020). Similar to the linear parameterisation, about half of the ESM-RF pairs has a calibrated melt sensitivity higher than the ISMIP6 AntMean range for the Amundsen calibration. These model pairs would have underestimated historical ice discharge in the Amundsen region if the ISMIP6 AntMean basal melt sensitivity had been applied.

For the quadratic parameterisation, the sensitivity of the calibration parameter to the thermal forcing is tested. In this way, the impact of the uncertainty in the reanalysis data set on the sea level projections is explored. This has been done by adding a positive temperature perturbation to the temperature time series near the ice shelf base of each ESM. The temperature perturbation is equal in size to one standard deviation between the reanalysis products (see the shaded orange regions in Fig 3). The resulting calibrated basal melt sensitivities are listed in Table 5 (Ice shelf base + 1σ). As expected, the higher ocean temperatures lead to stronger forcing in the quadratic parameterisation and therefore a lower basal melt sensitivity is required for the best fit with observations.

To summarise, a comparison of the ~~γ~~ calibrated basal melt sensitivity values in our study and ~~γ~~ equivalents in LARMIP-2 (Levermann et al., 2020) and ISMIP6 (Jourdain et al., 2020) suggests that calibration on past ice discharge rather than on basal melt observations results in relatively low ~~γ values~~ basal melt sensitivities for the Antarctic-wide calibration. The Amundsen ~~and Peninsula sector are~~ sector is more consistent with the high end of the ~~γ~~ basal melt sensitivity ranges applied in LARMIP-2

and the Antarctic mean calibration of ISMIP6~~, while the other sectors (EAIS, Ross, Amundsen) are more consistent with the lower end of those γ ranges~~. Furthermore, the spread in calibrated melt sensitivities is much higher than the observation-based ranges of LARMIP-2 and the ISMIP6 AntMean method. ESM-RF pairs with a strong thermal forcing over the historical period, will have a lower calibrated sensitivity than ESM-RF pairs with a weak thermal forcing to obtain the best fit with observed ice discharge. Models with calibrated melt sensitivity values outside the observation-based ranges would either underestimate or overestimate past ice discharge if observation-based sensitivities had been applied. As a result the spread in simulated ice discharge over the historical period will be lower for calibrated basal melt sensitivities than for the observation-based basal melt sensitivities.

~~Box-and-whisker plots of calibrated γ values of ESM-RF pairs. Only calibrated γ values greater than zero are shown in the plot. The percentage of ESM-RF pairs with positive γ values is indicated by the green values on top for each region. The horizontal green line indicates the median value, boxes indicate the 25-75 percentile range and whiskers the 5-95 percentile range. Values beyond this range are not shown. The shaded regions indicate γ ranges that are used in other studies. The green shading represents the γ values corresponding with the basal melt sensitivity range of 7-16 m yr^{-1} K^{-1} used in Levermann et al. (2020). The blue and yellow shading indicate the 5-95% range of the γ values used for the nonlocal quadratic parameterisation in ISMIP6 (Jourdain et al., 2020) for both the Antarctic mean (AntMean) and Pine Island Glacier (PIGL) calibration, respectively. For PIGL the 95% bound is 4.71 × 10^5, which is outside the scale of the vertical axis.~~

3.2 Hindcasts of Antarctic and Amundsen sea level contribution

Hindcasts of the ~~Antarctic dynamic contribution~~ dynamic contribution of the Amundsen region and the total AIS to sea level rise are made to assess how well ~~Rignot~~ changes in ice discharge could be reproduced after calibration over the period 1979-2017. The ~~total Antarctic sea level response is based on the summed contribution over the five sectors using the six calibrated basal melt computation methods (Table 3).~~ calibration is performed by fitting the sea level on observations using a least squares fit of the sea level contribution for each year, weighted equally, over the hindcast period. The results of the linear and quadratic parameterisation are about equal when applied to the region of calibration (same RMSE; Table 6). However, the quadratic parameterisation performs better (lower RMSE) after calibration on an independent region than the linear parameterisation (i.e. when calibrated on the Amundsen region and applied to the total AIS or vice versa). Additionally, the quadratic parameterisation is considered most realistic (Jenkins et al., 2018). In the remainder of this article, therefore, only results for the quadratic basal melt parameterisation are shown and discussed unless specified differently. Differences in the projections between the quadratic and linear parameterisation are further discussed in Sect. 3.3.2.

Figure 6 shows the hindcasts of all ~~combinations of CMIP6 models and LARMIP-2 linear response functions~~ ESM-RF pairs using the calibrated ~~γ values~~ basal melt sensitivities (Fig. 5). ~~Each panel represents a basal melt computation method~~ The two panels show the hindcasts for the total AIS and the Amundsen region, as specified ~~on top (Table 3).~~ in the titles. The total Antarctic sea level response is based on the summed contribution over the five sectors (Fig. 2). The colors represent two calibration methods, where red is the calibration on the Amundsen region and blue the Antarctic-wide calibration. The observed ice discharge values (Rignot et al., 2019) are shown in grey.

Table 6. RMSEs of the least squares fit of the median sea level contribution of each year, weighted equally, between calibrated results and ice discharge observations of Rignot et al. (2019). Results are shown for combinations of the two calibration methods (Amundsen and Antarctic-wide) and parameterisations (linear and quadratic) for two hindcast regions: AIS (AIS) and the Amundsen region.

Basal melt method	RMSE AIS [mm]	RMSE Amundsen [mm]
Linear Amundsen	14.9	1.4
Quadratic Amundsen	7.2	1.4
Linear Antarctic-wide	1.7	2.7
Quadratic Antarctic-wide	1.6	2.4
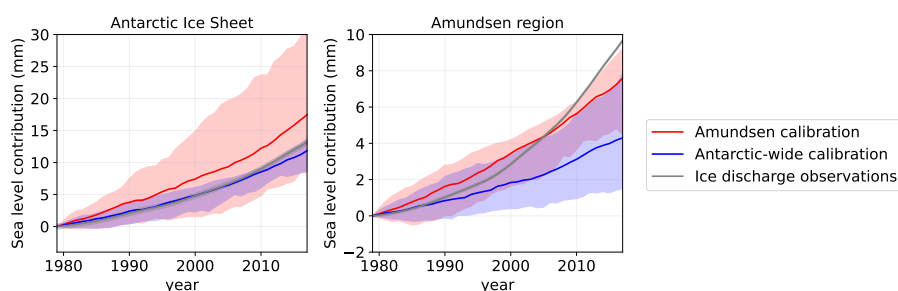
Figure 6. Impact of calibration target region on sea level illustrated by hindcasts showing the sea level contribution over the period 1979-2017 based on all calibrated ESM-RF pairs for the total AIS (left panel) and the Amundsen region (right panel). The historical experiment is extended with SSP2-4.5 scenario for the years 2015-2017. The red lines indicate the median contribution based on the regional Amundsen calibration, whereas the blue lines indicate the median contribution for the Antarctic-wide calibration. Only the quadratic parameterisation with thermal forcing near the ice shelf base is shown. The observation-based changes in ice discharge from Rignot et al. (2019) are shown in grey. The shaded area indicates the associated likely range (17th to 83rd percentiles) for the modelled response and the observational error for the Rignot et al. (2019) data.

First, we evaluate the cumulative magnitude of the modelled sea level contributions . Most ESM-RF pairs are not able to capture the magnitude of the summed Antarctic sea level contribution . For each method, the sea level over the period 1979-2017 (Table 7). The median Amundsen calibration overestimates the cumulative AIS contribution by about 30% whereas the median Antarctic-wide calibration underestimates the contribution by about 10%. For the Amundsen region, the cumulative contribution is underestimated by the median response . This underestimation can be largely attributed to the high number of γ values that were set to zero in the calibration procedure (Sect. 3.1) . For the unbounded calibrations (left and middle panels), the sea level response of the multimodel mean value over the 1979-2017 period is approximately half of the magnitude of the observed Antarctic value (Rignot et al., 2019). The median values of the bounded hindcasts (right panels) are closer to

355

360 ~~observations. This is because the calibrated γ value is greater than zero for each ESM-RF pair. Counter-intuitively at first notice, the linear bounded hindcasts (right panels) have a higher intermodel spread than the unbounded hindcasts. The bounded γ values, however, provide less freedom to restrict the historical response of individual ESM-RF pairs to observations, explaining the higher intermodel spread in the sea level contribution. Hindcasts of regional sea level contributions are further discussed in Appendix ??.~~ of the Amundsen calibration (ca. 20%) and strongly underestimated by the Antarctic-wide calibration (ca. 60%).

365 Both calibration methods do not give an agreement in terms of the cumulative sea level contribution because of the choice to calibrate on the time series rather than on the cumulative sum. Even though the Antarctic-wide calibration is (by construction) closer to the observed Antarctic ice discharge than the Amundsen calibration, the strong underestimation of the Amundsen region still means that the response in other regions is overestimated. It should be kept in mind that the errors in the individual regions compensate each other, resulting in a summed Antarctic response that is close to observations.

370 ### 3.3 ~~Selection of ESM-RF pairs~~

~~From the previous analyses we can conclude that for all basal melt computation methods most ESM-RF pairs are not able to capture the magnitude of the observed Antarctic~~ Second, we evaluate the evolution of the sea level response ~~to a reasonable extent. This makes them less trust-worthy for future projections of~~ over time. For the Antarctic-wide calibration, the median value overestimates changes in Antarctic discharge before 2001 and underestimates them thereafter. This means that the sea

375 level ~~response. Therefore, the calibration on ice discharge is combined with a model selection step in which ESM-RF pairs are selected that capture the summed Antarctic response. ESM-RF pairs are ranked based on their ability to simulate the magnitude of the observed Antarctic ice discharge over the 1979-2017 period. To compare the performance between the different methods, for each method the top 10% best-ranking ESM-RF pairs are selected. By taking the top 10%,~~ acceleration over the full period cannot be captured with the Antarctic-wide calibration, making it likely that it will be underestimated in future projections

380 as well. This is also visible in the ice discharge rate over the last decade of the hindcast (Table 7), which is lower than in observations. In a similar way, the Amundsen calibration overestimates the changes in Amundsen discharge before 2005 and underestimates them thereafter. So for the Amundsen region, even when using the Amundsen-specific calibration, the ~~same number of pairs (22)is selected for each method. The best models are defined as the ESM-RF combinations with the lowest RMSE compared to observed ice discharge over the full period. Figure ?? depicts the mean annual sea level contribution biases~~

385 ~~for this selection of ESM-RF pairs compared to the observations. The mean RMSE over the~~ acceleration is not captured by the median response and the rate over the last decade of the hindcast is underestimated. It should be noted that not just the acceleration of the Amundsen contribution cannot be reproduced, but also the relative dominance of Amundsen with respect to the total Antarctic contribution (about 70% in observations, about 30-40% in our results).

Since the Amundsen region is the most important contributing region to the summed Antarctic response over the hindcasting

390 period, we tested whether a selection of models could better capture past ice discharge in the Amundsen region. The top 10% ~~ESM-RF pairs is indicated in the legend and the inter-model spread is visualised for the best (QUA, lowest mean RMSE) and worst (LBR, highest mean RMSE) methods. The names of the~~ calibrated models with the best fit to ice discharge observations (Fig. A1) were selected for both the Amundsen and Antarctic-wide calibration. The selection was based on

the model performance in the calibration region. As a logical consequence, the top 10% ESM-RF ~~combinations for the best~~
~~method (QUA) are listed in Table ??. The LBR method has the highest mean RMSE due to the wide spread between individual~~
~~model combinations as explained in Sect. 3.2.~~

~~Although the model selection reproduces the summed Antarctic sea level response quite accurately, the acceleration in~~ ~~the observations is not well simulated (Fig. ??). On average,~~ pairs from the two calibration methods performs better on the cumulative sea level contribution in the calibration region (Table 7). Interestingly, the same selection of models also performs better in the ~~selected models overestimate Antarctic discharge before around 2010 and underestimate it thereafter.~~ ~~Furthermore, for individual regions the response is not always well captured (see e.g. Figures ?? and ?? for the QUA and QUR~~ ~~method, respectively). The spread in individual regions is higher~~ other region. After Antarctic-wide selection the Amundsen sea level contribution in the hindcasts are closer to observations. Unfortunately, for the Antarctic-wide ~~calibration~~ selection, the contributions of the other regions increase as well, which increases their error relative to observations. The Amundsen selection resulted in higher estimates than for the ~~regional calibration. Antarctic-wide calibration leads to regional responses~~ ~~that are overestimated in some regions and underestimated in others (Fig. ??) since the same γ is used for each region.~~ ~~Differences between Antarctic-wide and regional calibration are greatest for the Amundsen region , which is the most important~~ ~~contributing region to~~ full model suite in the ~~summed Antarctic response over the hindcasting period. The Amundsen and~~ ~~Peninsula contributions are underestimated by the selected models for the Antarctic-wide calibration. The EAIS response~~ ~~is reasonably well reproduced. The responses of the Ross and Weddell regionare slightly overestimated. The errors in the~~ ~~individual regions compensate each other, resulting in a summed Antarctic response that is well captured. For the regional~~ ~~calibration , the responses in individual regions are better captured and more restricted (Fig. ??).~~ Amundsen region itself (by construction), but lower estimates (closer to observations) for the Antarctic summed response. As a result, the Amundsen contribution relative to the total AIS improves after model selection on the Amundsen region. Nevertheless, also the mean response of the top 10% models could not reproduce the observed acceleration over the historical period in the Amundsen region. This means that despite its overestimation of the cumulative sum over the hindcast period for the AIS, the Amundsen calibration will presumably underestimate future projections of the sea level contribution for the Amundsen region.

~~Mean sea level contribution bias compared to observations of the top 10% ESM-RF pairs for each basal melt computation~~ ~~method. The numbers in the legend indicate the mean RMSE over the selected ESM-RF pairs over the period 1979-2017 in~~ ~~mm. The spread (standard deviation) of the top 10% models is indicated for the LBR (highest mean RMSE) and QUA (lowest~~ ~~mean RMSE) methods by the shading in the background.~~

3.3 ~~Projections~~Sea level contribution projections

In this section, projections of the ~~summed Antarctic~~ sea level contribution due to basal melt for the AIS and the Amundsen region are presented. The projections comprise the 21st century. Computations start in the year 1850 so that the delayed contribution of ice discharge to basal melt is included in the future sea level response. We assess two metrics: the cumulative magnitude and the rate of the sea level response. ~~The cumulative magnitude of the~~ The cumulative sea level response is ~~used~~ ~~to compare differences over the 21st century~~computed by taking the difference between the year 2100 and the average over

Table 7. ~~Hindcasts of CMIP6-forced~~ The median cumulative sea level ~~response~~ contribution (ΔS) over the hindcast period 1979-2017 ~~based on 14 CMIP6 models~~ and ~~16 linear response functions. The historical experiment is extended with SSP2-4.5 scenario for~~ the ~~years 2015-2017. The figure shows~~ rate (dS/dt) over the ~~results~~ last decade (2008-2017) of the hindcast period for the ~~full model suite of ESM-RF pairs~~ two calibration methods (~~green~~Amundsen and Antarctic-wide) ~~, together with~~ and for the ~~Rignot~~ ice discharge ~~(grey)~~observations of Rignot et al. (2019). ~~The shaded area indicates one standard deviation, representing intermodel spread~~ Results are shown for the ~~modelled response and observational error for~~ quadratic basal melt parameterisation with thermal forcing near ~~the Rignot data~~the ice shelf base.

Source	AIS		Amundsen region	
	ΔS [mm]	dS/dt [mm/yr]	ΔS [mm]	dS/dt [mm/yr]
Ice discharge observations	13.1	0.58	9.7	0.48
Amundsen calibration	17.5	0.84	7.6	0.27
Antarctic-wide calibration	11.8	0.45	4.3	0.17
Amundsen calibration - top 10%	16.6	0.86	9.3	0.44
Antarctic-wide calibration - top 10%	13.3	0.60	5.3	0.24

the period 1995-2014. The sea level response rate at the end of the 21st century is indicative of differences in committed sea level rise beyond 2100. The sea level response rate is computed by a linear regression on the sea level response over the period 2081-2100.

3.3.1 ~~Magnitude and rate~~

~~First,~~ First, we present the calibrated projections and explore the impact of calibration on projections of the ~~cumulative magnitude of the~~ sea level ~~response is analysed. The cumulative sea level response is computed by taking the difference between the year 2100 and the average over the period 1995-2014. Figure ??~~ contribution. Second, the sensitivity of projections to methodological choices, such as the parameterisation relation (quadratic/linear), thermal forcing depth (ice shelf base/800-1000 m) and model selection (Earth system model/Ice sheet model) is explored.

3.3.1 Impact of calibration on sea level projections

Figure 7 shows projections for the SSP5-8.5 scenario, based on the calibrated basal melt sensitivities for the quadratic parameterisation and thermal forcing near the ice shelf base. The Amundsen calibration leads to approximately 60% higher projections than the Antarctic-wide calibration, which can be attributed to the higher basal melt sensitivities for this calibration method (Fig. 5).

To understand how calibration of individual ESM-RF combinations on past ice discharge influences the results compared to using observation-based basal melt sensitivities, we also made projections in which a single basal melt sensitivity is applied in all ESM-RF combinations. This single value is the median basal melt sensitivity applied in LARMIP-2 (Levermann et al., 2020)
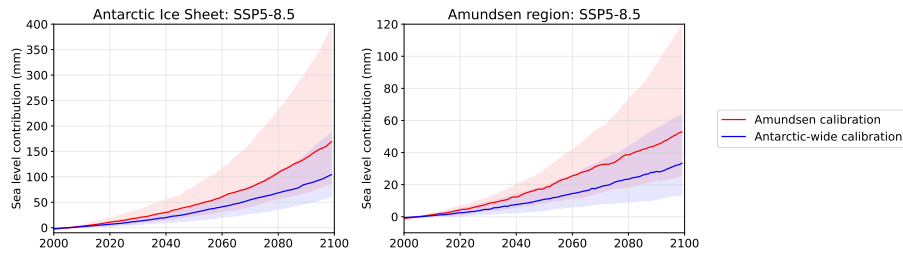
Figure 7. Projections showing the calibrated sea level contribution over the period 2000-2100 based on SSP5-8.5, for the total AIS (left panel) and the Amundsen region (right panel). The red lines indicate the median contribution based on the regional Amundsen calibration, whereas the blue lines indicate the median contribution for the Antarctic-wide calibration. Results are shown for the quadratic parameterisation and thermal forcing near the ice shelf base. The shaded area indicates the associated likely ranges (17th to 83rd percentiles).
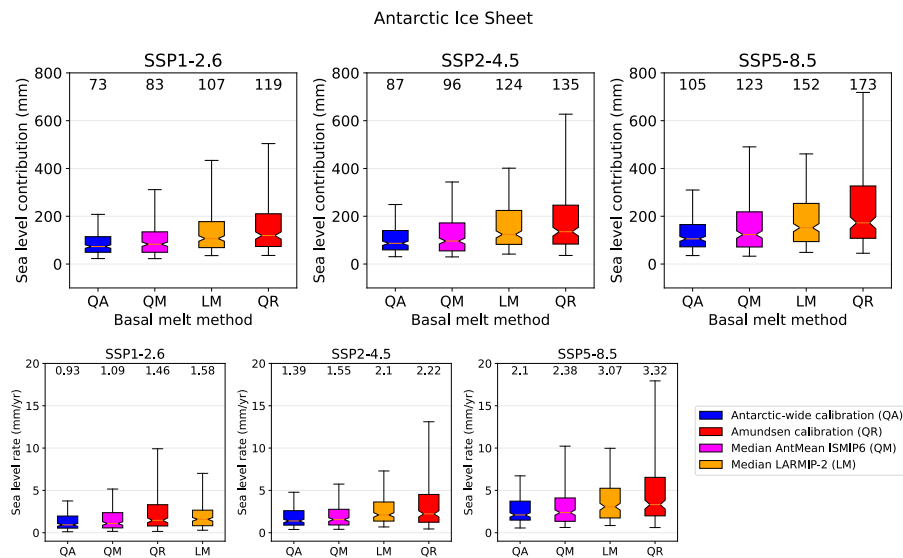
Figure 8. Projected Antarctic sea level response for SSP1-2.6, SSP2-4.5 and SSP5-8.5. Top panels show the sea level contribution in 2100 compared to the period 1995-2014 and bottom panels the sea level rise rates over the period 2081-2100. The spread is determined by the calibrated ESM-RF pairs. The black numbers indicate the median values (the orange lines), whereas the boxes show the 25-75 percentiles and the whiskers the 5-95 percentiles. The basal melt computation methods are ordered from the lowest to the highest median sea level response. ESM-RF pairs that could not be calibrated are removed from all basal melt methods so that the same models are included in the comparison. If ESMs did not simulate year 2100, 2099 was used instead.

for the linear parameterisation and the median nonlocal basal melt sensitivity applied in ISMIP6 for the AntMean method
445 (Jourdain et al., 2020) for the quadratic basal melt parameterisation.

First, the sea level contribution of the total AIS is analysed. Figure 8 shows the projected sea level response for each SSP scenario and different basal melt computation methods. The top panels represent the cumulative projections and the bottom panels the sea level response rate over the period 2081-2100. Not surprisingly a higher emission scenario leads to a higher sea level contribution. The SSP5-8.5 projections are almost 50% higher than the SSP1-2.6 projections. Absolute differences between the basal melt computation methods within one SSP scenario become more explicit for the higher emission scenarios, but relative differences (ratio of highest to lowest) are comparable.

The ratio of the highest to lowest basal melt method is only slightly larger than the ratio between the SSP5-8.5 and SSP1-2.6 scenario (averaged over all methods), indicating that the influence of the basal melt computation method on the sea level response is more or less similar to the impact of the emission scenarios. Since the highest basal melt method is the Amundsen calibration and the lowest method the Antarctic-wide calibration, this means that this difference can be entirely attributed to the calibration region.

The projections of the AIS using the median basal melt sensitivities applied in ISMIP6 and LARMIP-2 fall in between the two calibrated projections. This is consistent with the median basal melt sensitivity of LARMIP-2 and ISMIP6, which is located above the median Antarctic-wide calibrated value and below the Amundsen-calibrated value, respectively (Fig. 5). Even though

the spread between the basal melt methods is extended by using the calibration methods, using single basal melt sensitivities based on basal melt observations with different parameterisation types (linear/quadratic) also leads to a large spread in the projections. We remark that the top 10% best-performing models in reproducing ice discharge observations (Fig. A1), result in estimates that fall in between the Antarctic-wide (QA) and Amundsen calibration (QR) methods, reducing the spread (Fig. A2).

485

~~Same as Fig. **??** but for the sea level response rates over the period 2080-2100.~~

~~Second, the variation in the response rates is~~ As a next step, the AIS sea level response rates are assessed at the end of the 21st century (~~Table **??**~~2081-2100). These are important for sea level differences beyond 2100. The ~~response rate is computed by a linear regression on the sea level response over the period 2081-2100. The difference between the lowest and highest basal melt method~~ ratio of the highest to lowest median sea level rates of the different basal melt methods shows that the influence of the basal melt computation method on the response rate is ~~equal to or greater~~ smaller than the effect of the ~~emission scenario. By considering unbounded calibration methods only, the influence of the scenarios dominates over the basal melt computation method. The basal melt computation can be subdivided into calibration and parameterisation parts. The calibration step is the most distinctive feature in the basal melt computation. Antarctic-wide calibration results in higher projections than regional calibration.Bounded calibration gives higher values than unbounded calibration (comparison for the linear parameterisation only).~~SSP scenarios. The effect of the ~~parameterisation is smallest; The quadratic parameterisation provides higher estimates of future sea level rise~~ SSP scenarios is stronger for the quadratic parameterisations (QM, QA, QR) than for the linear one (LM). As a result the highest median response rate in SSP5-8.5 and SSP2-4.5 is using the QR basal melt method, whereas in SSP1-2.6 the response rate based on the median LARMIP-2 basal melt sensitivity (LM) is highest. This could be explained by the linear (rather than quadratic) relation with thermal forcing (see Sect. 3.3.2), which is independent on the absolute ocean temperature (which is linked to the SSP scenarios). It should also be noted that the Amundsen calibration is more skewed towards higher sea level response rates than the ~~linear parameterisation (comparison for the unbounded calibration only).~~ other basal melt methods. This could be explained by the higher basal melt sensitivities that were required to fit the modelled historical Amundsen sea level contribution to ice discharge observations.

505 ~~We conclude that sea level variations associated with basal melt computation methodsare equal or greater than variations between different pathways of future greenhouse gas emission scenarios. Within the basal melt computation methods, the calibration step is more important than the parameterisation type for the contribution of Antarctic ice discharge to~~ Second, the sea level ~~up to and beyond 2100.~~

3.3.2 ~~Best estimate~~

510 ~~In Sect. **??** the top 10% best ESM-RF pairs were selected based on their performance in reproducing observed Antarctic ice discharge over four decades. Figure **??** presents the projections of these selections. For each scenario, the top 10% selection shows on average a 20-28 mm higher median cumulative sea level response than the full model suite~~ projections of the Amundsen region are analysed (Fig. **??**). ~~This can be partly attributed to the fact that the selection does not include models with a γ of zero for the regions that contribute most (Amundsen , EAIS) to the sea level increase. Averaged over all basal melt~~
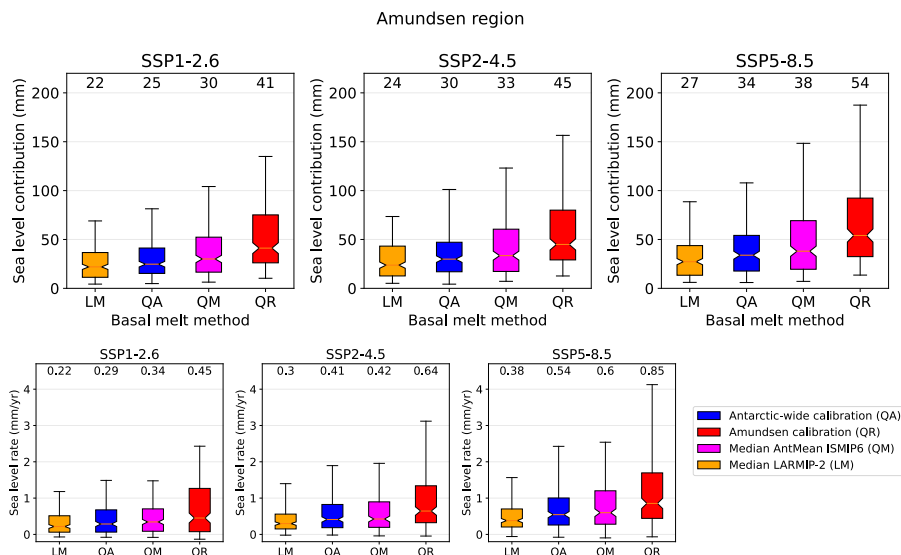
Figure 9. Same as Fig. 8 but for the Amundsen region.

515 ~~computation methods, 9).~~ For the Amundsen region, the highest projection is given by the Amundsen calibration, whereas the lowest projection is based on the median LARMIP-2 basal melt method. The ratio of the highest to lowest basal melt method is larger than the ratio between the SSP5-8.5 ~~has a median cumulative increase of 110 mm compared to 78 mm in~~ and SSP1-2~~.6.~~ ~~Furthermore, the different basal melt computation methods give more similar results for the selection than for the full model suite (Table **??**). In contrast to the full model suite, for the selection there is no clear relation between~~ .6 scenario (averaged

520 over all methods), indicating that the influence of the basal melt computation method ~~and the response magnitude within an emission scenario. For the top 10% selection the influence on the response magnitude~~ on the sea level response is larger than the impact of the emission scenarios. Also for the Amundsen sea level response rates, the impact of the basal melt ~~computation method is thus equal to or smaller than the effect of the emission scenario.~~

~~The top 10% selection shows on average 0.2-0.5 mm yr^{-1} higher sea level rates than the full model suite (Fig. **??**).~~ method

525 is slightly larger than the impact of the SSP scenario. However, the rate is much more sensitive to the SSP scenario than the cumulative sum. The rate is about 80% higher in SSP5-8.5 ~~has a median response rate that is about twice as large as the rate of~~ compared to SSP1-2.6~~. As for the cumulative contribution, the rates of the selected ESM-RF combinations are more equal between different basal melt computation methods for the model selection than for the full model suite~~, whereas the cumulative sea level contribution is only about 30% higher, indicating increasing differences between SSP scenarios beyond 2100.

530 The Amundsen calibration is considered to give the most realistic estimate for future projections of ice discharge in the Amundsen region. Considering the strong underestimation of past ice discharge rate in the Amundsen region using the Antarctic-wide calibration (Table **??**).~~For the top 10% selection the influence on the response rate of the basal melt computation method is smaller than the effect of the emission scenario. Different than for the full model suite, the selection consistently~~

~~shows higher sea level rates for the Antarctic-wide calibration than~~ 7), we expect that the future projections for the Amundsen region will be too low when using this method. The Amundsen projections using the median LARMIP-2 basal melt sensitivity (LM) are lower than for the ~~regional calibration. This can be explained by the higher contributions (higher γ) of the Ross and Weddell sectors, which show a clear warming trend in the subsurface ocean (Fig. 4). Other aspects (bounded vs unbounded calibration, quadratic vs linear parameterization)do not have a noticeable effect on~~ Antarctic-wide calibration method and therefore are also expected to underestimate the sea level contribution of the Amundsen region. The projection based on the median ISMIP6 sensitivity (QM) is probably also too low, since even the hindcasts based on the Amundsen calibration slightly underestimated observed ice discharge in the Amundsen region.

We conclude that for the AIS the cumulative sea level variations associated with basal melt computation methods are about equal to variations between different SSP scenarios. For the Antarctic sea level response rate, the SSP scenario is more important than the ~~response rate of the top 10% selection.~~ basal melt method. In contrast, for the Amundsen region the basal melt method impacts the projections (cumulative sum and rate) more than the SSP scenarios. For the Amundsen region, we also conclude that the Amundsen calibration probably gives the most reliable projections since the Amundsen calibration already underestimated past ice discharge and its acceleration in the hindcasts and the other methods give even lower estimates.

Furthermore, we compared our estimates with the emulated ISMIP6 and LARMIP-2 studies as presented in IPCC AR6 (Table 8). Despite the different method applied, the resulting projections of Antarctica's sea level contribution are in line with previous multi-model studies (ISMIP6, LARMIP-2). The Amundsen calibration results in an estimate that sits more or less in between the ISMIP6 and LARMIP-2 projections, as presented in IPCC AR6 (Fox-Kemper et al., 2021). It should be noted that this can only partly be attributed to the calibration on ice discharge observations, since the projections using the median ISMIP6 AntMean sensitivity (QM) and the median LARMIP-2 sensitivity (LM) result in lower estimates than for ISMIP6 AR6 and LARMIP-2 AR6, respectively. The differences with ISMIP6 and LARMIP-2 will be further discussion in Sect. 4.

~~For the top 10% of each basal melt computation method,~~

3.3.2 Impact of methodological choices on projections

In this section we explore what the impact is of several methodological choices on the sea level response projections of the AIS and Amundsen region. These choices include the parameterisation relation (quadratic/linear), thermal forcing depth (ice shelf base/800-1000 m) and model selection (Earth system model/Ice sheet model). Additionally, we further motivate our choices to use the quadratic parameterisation ~~combined with an~~ with thermal forcing near the ice shelf base in our main projections (Fig. 7; QA and QR in Figs. 8 and 9).

First we assess the impact of the parameterisation type on the calibrated projections for the AIS and the Amundsen region (Fig. 10). To this end we applied two different parameterisations: a linear and a quadratic relation with thermal forcing. Both relations are calibrated on observed ice discharge (Fig. 5) using the Antarctic-wide ~~calibration (QUA) resulted in the best estimate of Antarctic discharge over almost four decades (lowest overall RMSE)(Sect. 3.2)~~ and the Amundsen calibration. The results show that if the parameterisation is used to make projections for the same region as the region that is used for calibration the cumulative sea level contribution is almost equal for both parameterisations. This means that calibration on past

Table 8. ~~Similar~~ Projected dynamic contributions to ~~Table ??~~ sea level in meters from the AIS in 2100 relative to 1995-2014. The numbers for LARMIP-2, ~~but~~ ISMIP6 and SMB are obtained from the IPCC AR6 report (Fox-Kemper et al., 2021). Note that ~~for the sea level response rate over 2081-2100~~ ISMIP6 estimate surface mass balance contributions are removed as our study only accounts for changes in ice discharge.

Scenario	Forcing/Source	17%	
~~Variable~~ SSP5-8.5/RCP8.5	~~Condition~~ Antarctic-wide calibration (QA)	~~Variation in source variable~~ 0.06	~~Variation fact~~
~~Scenario~~	~~All~~ Amundsen calibration (QR)	~~SSP1-2.6 -> SSP5-8~~ 0.09	
	Median ISMIP6 sensitivity (QM)	0.05	
	Median LARMIP-2 sensitivity (LM)	0.08	
	ISMIP6 AR6 (excl. SMB)	0.10	
	LARMIP-2 AR6	0.10	
SSP2-4.5/RCP4.5	~~1.9-2.6~~ Antarctic-wide calibration (QA)	0.05	
~~Scenario~~	~~Top 10%~~ Amundsen calibration (QR)	0.07	
	Median ISMIP6 sensitivity (QM)	0.04	
	Median LARMIP-2 sensitivity (LM)	0.06	
	ISMIP6 AR6 (excl. SMB)	0.07	
	LARMIP-2 AR6	0.09	
SSP1-2.6 ~~SSP5-8.5~~/RCP2.6	~~1.9-2.5 Basal melt computation~~ Antarctic-wide calibration (QA)	~~All~~ 0.04	~~Lowe~~
~~Basal melt computation~~	~~Top 10%~~ Amundsen calibration (QR)	~~Lowest -> Highest~~ 0.06	
~~Basal melt computation~~	~~Unbounded calibration~~ Median ISMIP6 sensitivity (QM)	~~Lowest -> Highest~~ 0.04	
~~Calibration region~~	~~All~~ Median LARMIP-2 sensitivity (LM)	~~Regional -> Antarctic~~ 0.06	
~~Calibration bounds~~	~~All, Linear parameterisation~~ ISMIP6 AR6 (excl. SMB)	~~Unbounded -> Bounded~~ 0.06	
~~Parameterisation~~	~~All, Unbounded calibration~~ LARMIP-2 AR6	~~Linear -> Quadratic~~ 0.08	

ice discharge strongly constrains the future response if applied to the region of projections. ~~If reproducing the past is good indicator for making future projections, this basal melt computation method (QUA) will arguably provide the best estimate for the sea level contribution of Antarctic discharge over the coming century. We compared our best estimate with the emulated ISMIP6 and~~

On the other hand, if the calibration is performed in the Amundsen region and applied to make Antarctic projections, or vice versa, clear differences between the linear and quadratic relation appear. For the Amundsen calibration, the quadratic parameterisation results in lower projections for the Antarctic-wide contribution than the linear parameterisation. This can be expected, since the quadratic parameterisation is dependent on the absolute ocean temperature, whereas the linear parameterisation only uses temperature anomalies. By its definition the quadratic relation with thermal forcing implies that sectors that are melted by warmer waters are more sensitive than the colder sectors, even if the same basal melt sensitivity is applied. So if the Amundsen calibration is applied to colder ocean sectors, this leads to less basal melt for a similar temperature increase,
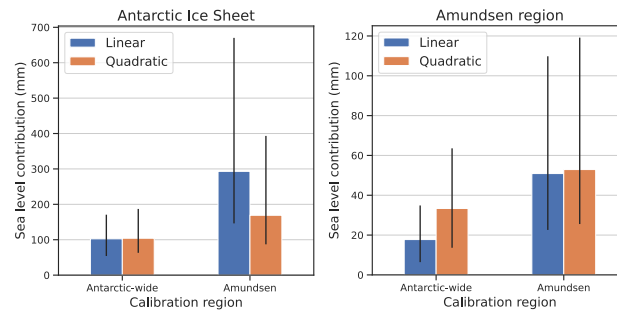
Figure 10. Projections of Antarctic sea level contribution for SSP5-8.5 for all calibrated ESM-RF combinations for the AIS (left) and Amundsen region (right). Results are shown for thermal forcing near the ice shelf base. The bars show the median projections for the Antarctic-wide and regional Amundsen calibration using the quadratic (orange) and linear (blue) parameterisations. The spread indicates the 17th to 83rd percentiles.

since the ocean temperatures are lower. The linear relation is independent of the absolute temperature, and therefore cannot
580 be calibrated in one sector and then applied to another one. For the Amundsen calibration, the linear basal melt sensitivity will be too high for the Antarctic-wide projections and lead to an overestimation of the Antarctic response since the sensitivity is completely accounted for by the γ parameter. In a similar way, Antarctic-wide calibration of the linear parameterisation leads to an underestimation of the basal melt sensitivity and thus lower projections for the Amundsen region than the quadratic parameterisation. We conclude that for the linear calibration basal melt sensitivities can only be calibrated on the projection
585 region. The quadratic relation can be better used when calibrating on (partly) independent regions since it is dependent on the absolute ocean temperature, which is an important motivation to apply the quadratic parameterisation in our study.

Second, we assessed the impact of the thermal forcing depth on the calibrated projections (Fig. 11). For this experiment, thermal forcing and basal melt sensitivity are based on ocean temperature at two different depths: 100 m centered around the mean depth of the ice shelf base (similar to LARMIP-2 ~~studies as presented in IPCC AR6~~) and an ocean layer around the
590 depth of the continental shelf near the ice shelf front. The deeper ocean layer is chosen for comparison since the relevant water masses that drive the melting close to the grounding line origin from the deepest depth of the bed near the ice shelf front, which we approximate as 800-1000 m. We only use the quadratic parameterisation, which is dependent to the absolute ocean temperature. Surprisingly, for the deeper layer, the Antarctic-wide calibration leads to a lower basal melt sensitivity, whereas the Amundsen calibration leads to a higher basal melt sensitivity than the corresponding basal melt sensitivities near
595 the ice shelf base (Table ~~8). The cumulative sea level response is equal or smaller in magnitudethan emulated ISMIP6 estimates across all scenarios (depending on the basal melt computation method). Compared to LARMIP-2, the response is smaller. The differences with ISMIP6 and LARMIP-2 can be mainly attributed to the calibration on past ice discharge, which resulted in less sensitive basal melt parameterisations (Fig. 5).~~ 5). This can be explained by the differences in the water temperature and the warming rates of the two layers. For the Amundsen region, the ocean temperature in the deeper 800-1000 m layer warms
600 slower than the ocean temperature near the ice shelf base (Fig. A3), although the temperature itself is comparable in magnitude.
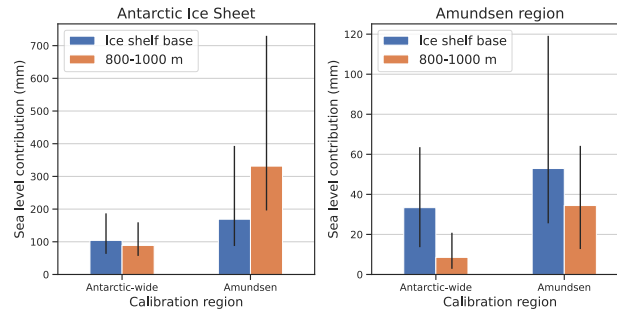
Figure 11. Projections of the sea level contribution of the AIS (left) and Amundsen region (right) for SSP5-8.5 for all calibrated ESM-RF combinations using the *quadratic* parameterisation. The bars indicate the median sea level contribution in 2100 relative to 1995-2014. The thermal forcing and basal melt sensitivity are based on ocean temperature at two different depths: 100 m centered around the mean depth of the ice shelf base (blue) and 800-1000 m depth (orange). The black lines indicate the 17th to 83rd percentiles.

Therefore, a higher basal melt sensitivity is required to match ice discharge observations. In contrast, for all other regions, the ocean layer at 800-1000 m depth is warmer than the temperature near the depth of the ice shelf base, resulting in a higher ocean forcing. In the Weddell, Ross and the Peninsula regions, the temperature also warms faster in the deeper layer than in the layer at the depth of the ice shelf base, resulting also in stronger ocean forcing. As a consequence, the calibrated basal melt

605   sensitivity is lower for the Antarctic-wide calibration.

For the AIS projections, the lower Antarctic-wide basal melt sensitivity for 800-1000 m depth is largely compensated by a larger ocean forcing for the Antarctic-wide calibration. This results in a similar sea level contribution for the 800-1000 m-based projections compared to using the thermal forcing near the depth of the ice shelf base. However, the high Amundsen basal melt sensitivity for the 800-1000 m depth combined with the larger Antarctic-wide ocean forcing leads to higher estimates for the

610   AIS projections. Projections for the Amundsen region are oppositely affected. The ocean forcing is smaller at 800-1000 m depth than near the ice shelf base, and combined with a lower basal melt sensitivity for the Antarctic-wide calibration this leads to much smaller projections. For the Amundsen region itself, the higher basal melt sensitivity partly compensates for the smaller ocean forcing, resulting in a smaller sea level projection. As a result, the fraction of Amundsen compared to the total Antarctic contribution is larger for the thermal forcing near the ice shelf base than for the 800-1000 m depth layer. Since

615   this fraction was already smaller than in observations in the hindcast experiments using thermal forcing near the ice shelf base (Sect. 3.2), we argue that using thermal forcing near the ice shelf base leads to more realistic results than thermal forcing in the 800-1000 m depth layer.

We conclude that the depth of thermal forcing has a large influence on the resulting sea level contribution in future projections. Most straightforward, it influences the thermal forcing in the projections, which is depth-dependent, but also region-dependent.

620   However, when calibration is applied, the thermal forcing depth also affects the strength of the basal melt sensitivity through

its evolution over the historical period. The thermal forcing near the ice shelf base leads to a more realistic contribution of the Amundsen region compared to the total AIS, and is therefore applied throughout this study.

3.3.3 Modelling uncertainties associated with Earth System and Ice Sheet Models

In this section, we assess the role of CMIP6 ESMs and RFs of the LARMIP-2 ice sheet models in projection uncertainties for the AIS by comparing the projected sea level contributions for the Amundsen calibration, which is considered to perform better than the Antarctic-wide calibration (see Sect. 3.3.1). These models cause the spread of the projections for a specific basal melt method (see the shaded regions in Fig. 7 and the error bars in Figs. 8-11). Fig. 12 shows the projected Antarctic sea level contribution for each individual CMIP6 ESM for the Amundsen calibration. Here, the spread for each ESM is determined by the linear response functions of the ice sheet models. Noticeably, the differences between the scenarios are small compared to the differences between individual ESMs, despite the bias adjustment with ocean reanalysis data. As a measure of ESM spread, we compute the standard deviation between the median values (bar heights). The intermodel standard deviation varies from 144 mm for SSP1-2.6 to 205 mm for SSP5-8.5.

The ESM with the strongest median sea level contribution (CAS-ESM2-0) also exhibits the largest warming over the 21st century for each individual ocean sector and has the second highest median calibrated basal melt sensitivity for the Amundsen region (not shown). Also, it has the fourth lowest ranking in reproducing historical ice discharge compared to the other ESMs. Remarkably, the five ESMs with the highest RMSE for the Amundsen region (when comparing their historical performance to ice discharge observations) are amongst the six models with the highest cumulative sea level contribution for the AIS in the projections. This suggests that applying ESM selection based on the performance of ESMs in reproducing ice discharge observations in the Amundsen region would result in lower estimates of the Antarctic dynamics contribution to sea level projections.

Similar to Fig. 12, Fig. 13 shows the projected Antarctic sea level contribution for the RF of each individual ice sheet model. Here, the spread in the error bars is determined by the CMIP6 ESMs. The RF spread is also greater than the scenario-induced spread. Similar as for the ESMs, we computed the intermodel standard deviation between ice sheet models as a measure of ice sheet model spread. The standard deviation between the median values varies from 46 mm for SSP1-2.6 to 62 mm for SSP5-8.5.

The RF of the ice sheet model giving the smallest median sea level contribution (GRIS LSC) has the second lowest calibrated basal melt sensitivity for the Amundsen region and could not be calibrated in combination with half of the ESMs. We remark that this RF also gave the smallest signal in LARMIP-2 (Levermann et al., 2020). The RF of the ice sheet model with the smallest calibrated basal melt sensitivity (PISM DMI) also could not be calibrated when combined with the forcing for 6 out of the 14 ESMs. Moreover, GRIS LSC and PISM DMI have the highest RMSE when compared with observed ice discharge.
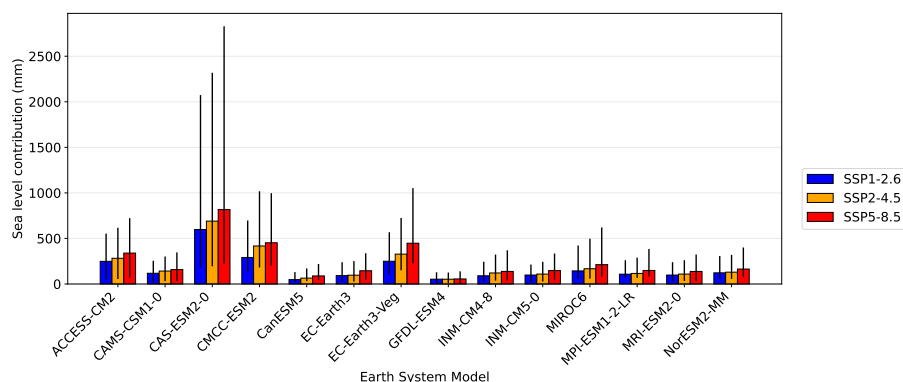
Figure 12. Projected Antarctic sea level changes for SSP1-2.6 (blue), SSP2-4.5 (orange) and SSP5-8.5 (red) over the 21st century, defined as the difference between year 2100 and the period 1995-2014. For each CMIP6 ~~model~~ESM, the errorbars indicate ~~one standard deviation between~~ the 17th to 83rd percentiles (computed from the associated RF timeseries). Basal melt is computed with the quadratic parameterisation which is calibrated ~~Antarctic-wide (QUA)~~on the Amundsen region.

655   This suggests that RF selection based on reproducing historical ice discharge would result in higher future estimates of the sea level contribution~~by a factor 12.7 (14.3).~~.

     As a final assessment, the RMSE over the Amundsen region was used to rank the historical performance of individual combinations of ESM-RF pairs. The top 10% best-performing ESM-RF pairs have slightly lower estimates for the Antarctic contribution but similar estimates for the Amundsen contribution (Fig. A2). As a result the relative contribution of the Amundsen

660   region increases compared to the total Antarctic dynamics contribution to sea level, as was also visible in the hindcasts of the top 10% models (Table 7).

     This assessment shows that modelling uncertainties of ESMs as well as ice sheet models are a greater source of uncertainties in Antarctic mass loss projections than the emission scenarios and the basal melt computation methods applied in this study. The uncertainties associated with the ocean temperature evolution from ESMs is even larger than those from ice sheet models,

665   despite the bias adjustment that has been applied to the subsurface temperatures. We also find some relations between historical model performance and future projections, which point at model selection as a potential next step to better understand the future contribution of Antarctic dynamics to sea level changes.

4   Discussion

     In this study, ~~calibrated projections of Antarctica's~~ projections of the dynamic sea level contribution ~~were made that are~~

670   ~~consistent with~~ of the AIS and the Amundsen region are presented that were calibrated on four decades of ~~past ice discharge in~~ ice discharge observations. Calibration was applied on the basal melt parameterisation. The contribution of Antarctica's ice discharge to sea level changes is computed ~~with~~ using forcing from state-of-the-art ESMs from Coupled Model Intercomparison Project Phase 6 (CMIP6) ~~and~~ applied to linear response functions from LARMIP-2 ice sheet models. The major strength
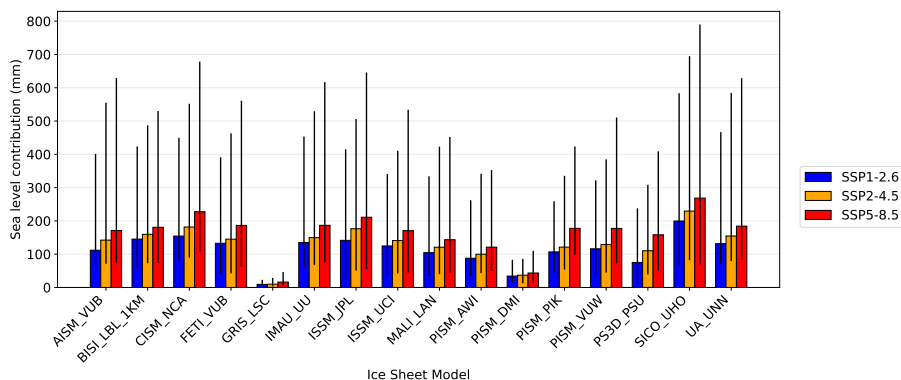
Figure 13. Projected Antarctic sea level changes for SSP1-2.6 (blue), SSP2-4.5 (orange) and SSP5-8.5 (red) over the 21st century, defined as the difference between year 2100 and the period 1995-2014. For each RF, the errorbars indicate ~~one standard deviation between~~ the 17th to 83rd percentiles (computed from the associated ~~CMIP6 models~~ESMs). Basal melt is computed with the quadratic parameterisation which is calibrated ~~Antarctic-wide (QUA)~~on the Amundsen region.

of this method is that multiple climate and ice sheet models can be combined to assess ~~the~~ their full range of modelling uncertainties. A drawback of the method is that non-linearities between thermal forcing and ice sheet mass loss, related to ice sheet instabilities and ocean dynamics are not considered because we use the ~~Linear Response Functions framework. Our results show that the models that we used, even the top 10%, are not able~~ linear response functions framework.

The inability of our models to represent the ~~acceleration present in the observations~~ observed acceleration (Fig. **??**) ~~, with overestimation of mass loss before 2010 and underestimation thereafter. This~~ 6) could be explained by ice sheet/ocean feedbacks that are not represented in the models. Recent studies suggest a positive feedback between ice sheet melting and subsurface ocean warming (Bronselaer et al., 2018; Golledge et al., 2019; Sadai et al., 2020) that could explain this deficiency in the models. One reason to introduce the quadratic parameterisation was to account for ~~some~~ a positive feedback between ice melt and ocean forcing, as presented in Jenkins et al. (2018). However the feedback between surface freshening due to melt water and basal ice shelf melt is not explicitly simulated ~~. Recent studies suggest that this feedback is positive (Bronselaer et al., 2018; Golledge et al., 2019; Sadai et al., 2020), which could explain the inability of our models to represent the observed acceleration~~in this parameterisation. It should also be noted that our study does not address the impact of surface melt on calving nor marine ice cliff instability processes, which means that the projections are a lower bound of what could happen in reality.

~~Temperature-melt~~ In the current generation of ESMs (CMIP6) ice shelf cavities are not (fully) represented, leading to deficiencies in the process representation (Mathiot et al., 2017). The inflow/ambient temperature is affected by mixing with meltwater and ocean dynamical processes inside the cavity. Furthermore, pressure changes inside the cavity impact the freezing point temperature and thus the thermal forcing. Also, the resolution of most CMIP6 ESMs is not high enough to resolve the ocean circulation on the continental shelf, including the Antarctic Slope Current (Thompson et al., 2018). Due to these ocean

model deficiencies, temperature-melt relations are typically parameterised in terms of the heat exchange velocity γ (Favier et al., 2019)~~.~~, which is used as calibration parameter in our study.

The region of calibration is relevant for the projections, since the ~~calibrated γ value~~ basal melt sensitivity varies around the continent and is dependent on the ice-shelf cavity type. Calibration of the γ value in the basal melt parameterisation results ~~regularly~~ for 10-17% of the ESM-RF pairs in a value of zero, ~~especially for the Weddell and Ross regions. A γ value of zero~~ which indicates insensitivity of basal melt to open ocean subsurface temperature changes. ~~The likeliest explanation would be that the models predict a warming while the observed discharge decreased over the observation period (or vice versa).~~ This could be caused either by the importance of natural (multidecadal) variability in the ~~observations or~~ ice discharge observations and/or simulated ocean forcing or by the inability of the ESMs to simulate temperature trends around Antarctica. ~~Furthermore, the observed ice discharge trend could be close to zero (for the Weddell sector) . Another explanation~~ However, we found that each ESM could lead to a successful (positive γ) calibration if combined with several RFs, so it is the ESM-RF combination which determines whether calibration is successful. A physical explanation for a mismatch is that the water inside the ice shelf cavities is blocked from the water in the coastal region outside the cavities due to density gradients. This contradicts the assumption in this study that water from the open ocean can freely access the ice shelf cavities. Also note that the ocean sectors in our study are somewhat wider than the continental shelf, consistent with Levermann et al. (2020). The advantage of a wider region is that it allows for more assimilated observations in the reanalysis product that is used for the bias adjustment of ocean temperature (the continental shelf region is only sparsely sampled).

It is questionable whether the situation during the calibration period is representative for the future. In the future model projections (Fig. 4), especially for SSP5-8.5, all coastal regions, especially the Weddell and Ross sectors, experience a warming signal. As the open ocean outside the cavities warms, it could be expected that this warming will at a certain moment also be transported inside the cavities, and contribute there to basal melt and ice discharge. New calibration will then lead to ~~γ values that are greater than zero~~larger Antarctic-wide basal melt sensitivities. This means that calibrated ~~γ values~~ basal melt sensitivities that link open ocean subsurface temperatures outside cavities to basal melt underneath ice shelves could be ~~climate-state dependent~~time-evolving. It should also be noted that we calibrated the basal melt parameterisation based on basal melt anomalies and not on absolute basal melt. This is because that allows us to better represent observed melt but the downside is that anomalies are a second order effect that is harder to model ~~. Lastly, in the current generation of ESMs (CMIP6) ice shelf cavities are not (fully) represented, leading to deficiencies in the process representation (Mathiot et al., 2017).~~ and observe.

In this study, an Antarctic-wide and regional Amundsen calibration of the basal melt parameterisation have been applied. ~~Arguably, the regional parameterisation is more physically correct since individual regions might respond differently to similar forcing due to differences in ice and ocean dynamics and ice geometries. However, for the Ross, Weddell and Peninsula regions, 50-84% of the ESM-RF combinations have a calibrated γ equal to zero, resulting in no sea level contribution in future projections. For these regions, regional calibration leads to lower median contributions than Antarctic-wide calibration. A possible~~ The relation between thermal forcing and basal melt is more difficult to derive for the full AIS. The reason is that ~~these regions have no clear ocean temperature trend over the period 1850-2018 (and thus small thermal forcing) and relatively small changes in~~ it includes regions in which ocean warming has not been causally linked to changes in ice dynamics as the

warming was too small or absent over the historical period. However, regions with small ice discharge during the calibration period ~~. Calibrating~~ are expected to melt as the climate warms. The calibration could therefore result in a basal melt sensitivity which is too low for future projections. Moreover, calibrating on the Antarctic-wide response gives a less accurate reproduction of the historical mass loss in ~~these regions, but arguably a better prediction of future mass loss (when the ocean is warming in these regions). Also, it should~~ the Amundsen region. Therefore, the Antarctic-wide calibration gives information about a lower bound for the future projections: i.e. what would happen if the total AIS would keep the same basal melt sensitivity to ocean warming in the future.

The Amundsen region is considered the best region for calibration since it has been shown that the Amundsen mass loss is dominated by ice dynamics. Previous studies have shown that ice dynamical changes were causally linked to ocean warming during the observational record (Rignot et al., 2019). It could be expected that when ocean temperatures increase and experience similar warming rates in other regions, the basal melt sensitivity will also increase in those regions. It should also be noted that the quadratic parameterisation does introduce some regional difference in basal melt sensitivity ~~, with~~ due to its dependence on the absolute temperature, resulting in a lower sensitivity in colder cavities. ~~Since both calibration methods have their advantages and disadvantages, we applied and compared both calibration methods.~~

~~Projected dynamic contributions to sea level in meters from the Antarctic ice sheet in 2100 relative to 1995-2014. The numbers for LARMIP-2, ISMIP6 and SMB are obtained from the IPCC AR6 report (Fox-Kemper et al., 2021). Note that for the ISMIP6 estimate surface mass balance contributions are removed as our study only accounts for ice discharge. QUA and LBA are shown as the best-performing method in reproducing hindcasts (QUA) and the method that is most comparable to the LARMIP-2 experiment, but calibrated on past ice discharge (LBA) (Fig. ??).. Scenario Forcing/Source 16.6% 50% 83.3%SSP5-8.5/RCP8.5 Selected models / QUA 0.10 0.12 0.13 Selected models / LBA 0.10 0.12 0.14 ISMIP6 excluding SMB 0.10 0.13 0.17 LARMIP-2 0.10 0.20 0.39SSP2-4.5/RCP4.5 Selected models / QUA 0.08 0.09 0.10 Selected models / LBA 0.06 0.10 0.12 ISMIP6 excluding SMB 0.07 0.12 0.16LARMIP-2 0.09 0.17 0.33SSP1-2.6/RCP2.6 Selected models / QUA 0.07 0.08 0.09 Selected models / LBA 0.07 0.08 0.10 ISMIP6 excluding SMB 0.06 0.11 0.15LARMIP-2 0.08 0.15 0.29~~

~~Each basal melt parameterisation method has been calibrated on ice discharge. For two basal melt computation methods (LBA, LBR) additional calibration has been performed on basal melt itself by setting observation-based bounds on the calibration parameter γ. The results show that basal-melt constrained (bounded) projections (LBA, LBR) lead to higher sea level estimates than their unconstrained (unbounded) counterparts (LUA, LUR). The main reason for this is that for~~ When the high basal melt sensitivities derived from the Amundsen calibration are applied to the other regions, the resulting basal melt will thus be smaller due to the colder temperatures. Arguably, the quadratic parameterisation based on the ~~bounded calibration γ values are greater than zero for all ESM-RF pairs, whereas for the unbounded calibrationonly 16-85% of the ESM-RF pairs have values greater than zero (~~Amundsen region is therefore more physically correct than the linear parameterisation. The nonlinear relation between melt and temperature change found in observations (Jenkins et al., 2018) also suggests that the quadratic relation based on the Amundsen region might be applicable to the cold-water sectors. The Amundsen calibration is therefore considered more reliable for future projections of the total AIS than the Antarctic-wide calibration. However,

individual regions might still respond differently to similar forcing due to differences in ice and ocean dynamics and ice geometries.

765 The AIS projections using our methodology with median MIP sensitivities (LM, QM; Fig. 5) . Parameter constraints on the heat exchange velocity γ in the bounded calibrations were obtained from the basal melt sensitivity parameter from the Levermann et al. (2020) range of 7-16 m yr^{-1} K^{-1}. Therefore it is interesting to compare the sea level contribution projections of the linear bounded Antarctic (LBA) calibration method with the LARMIP-2 projections over the same period (8) resulted in lower projections than in the original MIPs as presented in IPCC AR6 (Table 8). The Antarctic-wide calibration is compared 770 since differences between the AIS projections using our methodology with median MIP sensitivities and the original MIPs can be attributed to differences in thermal forcing and modelling of the ice sheet response. We used a different set of ESMs, which can lead to large differences in the modelled response (see Sect. 3.3.3). These large intermodel differences in ESMs point at model selection as a promising next step to reduce uncertainties in future projections of the contribution of ice dynamics to sea level changes. Since we only used temperature anomalies from ESMs as forcing, the selection criteria should not be based on 775 the mean climate but on climate trends. Furthermore, LARMIP-2 also applies the same basal melt sensitivity in each region. In LARMIP-2 the median projected sea level contribution is 0.15 m for RCP2.6 and 0.20 m for RCP8.5, compared to 0.08 m for SSP1-2.6 and 0.12 m for SSP5-8.5 in our study. The calibrated basal melt sensitivity (based on the associated calibrated γ value, Fig. 5) in our study has a median value of 7 m yr^{-1} K^{-1} for all calibration regions, except for the Amundsen sector, which has a median basal melt sensitivity of 12 m yr^{-1} K^{-1}. Also, Antarctic-wide calibration resulted in a median γ of 780 7 m yr^{-1} K^{-1}, this is the lower bound of the basal melt sensitivity range. Note that these values are different than the medians in Fig. 5 since here all ESM-RF pairs are included (as they all have positive values by definition) while Fig. 5 only includes a percentage of the models (those with positive γ values). This means that the randomly drawn γ values from the full range in the Levermann et al. study result on average in a more sensitive basal melt parameterisation than the calibrated γ values in our study and suggests that their basal melt sensitivity range should be revised downward to be consistent with past ice discharge. 785 Here, it should also be noted that LARMIP-2 overestimates the mass loss observations of Shepherd et al. (2018). The same argument applies to the uses global mean temperature as driver of the method, whereas we use bias-adjusted ocean temperature from the ESMs. The methodological differences with ISMIP6 γ-values. Similar to LARMIP-2, calibration shows that γ values in the lower bound of the Antarctic mean range applied in ISMIP6 are more consistent with four decades of past Antarctic ice discharge (Fig. 5). Consistent with the higher melt sensitivity the projected sea level contributions are therefore higher in AR6 790 are even larger than for LARMIP-2 and since ISMIP6 .

A short assessment was made on the role of CMIP6 ESMs and LARMIP-2 does not use the linear response functions framework but runs offline ice sheet models in projection uncertainties by comparing the median projected sea level contributions for the basal melt computation method with the best performance in the hindcasts (QUA) (Sect. 3.3.3). This assessment shows that modelling uncertainties, especially those related to ocean temperature evolution from ESMs, are a greater source of 795 uncertainty in to account for the ice sheet response. Despite all these differences in methodology, we arrive at projections which are in line with previous multi-model assessments of the contribution of Antarctic mass loss projections than the emission scenarios and the basal melt computation method. These large intermodel differences in ESMs as well as RFs explain why

~~model selection is essential to make future projections more consistent with observations of past ice discharge~~to future sea level. However, it could be expected that calibration of the basal melt parameterisation in ISMIP6 and LARMIP-2 on the Amundsen region will result in higher projections of the Antarctic sea level contribution than the projections presented in IPCC AR6.

5 Conclusions

This study presents calibrated projections of the contribution of Antarctica's ice discharge to sea level in 2100 compared to present-day (1995-2014). Since there is still high uncertainty in the temperature-basal melt relation (Dinniman et al., 2016), we applied a new approach to constrain this relation (Fig. 1). This was done by calibrating the modelled response on ice discharge observations rather than observation-based estimates of basal melt. Ocean thermal forcing is based on regional subsurface ocean temperature from 14 CMIP6 ESMs and 3 SSP scenarios and bias-adjusted with GREP ocean reanalysis data. ~~Basal melt is computed with a linear and quadratic relation with ocean thermal forcing. The ice discharge is~~ The changes in ice discharge are calculated with 16 linear response functions (RF) based on ice sheet model experiments from LARMIP-2. ~~New compared to other studies is the calibration of the modelled response. We applied a different, iterative approach to calibrate the basal melt computation (Fig. 1) since there is still high uncertainty in the temperature-basal melt relation (Dinniman et al., 2016). Past observations of ice discharge rather than basal melt are used for~~

An improvement over previous multi-model assessments, which focused mainly on the future, is that the new projections of the sea level contribution of Antarctic dynamics are more consistent with historical ice discharge observations. Calibration of individual ESM-RF pairs increased the spread in basal melt sensitivities but decreased spread in the hindcast experiments of Antarctica's sea level contribution. Unfortunately, calibration of the ~~melt parameterisation. The calibrated γ value for each individual ESM-RF pair is the one that is most consistent with four decades of observed ice discharge (Rignot et al., 2019). Apart from the bounded calibrations, the only (physical) limitation is that γ should be greater or equal to zero. Finally a top 10% selection of ESM-RF combinations is made, based on their performance~~ basal melt relation on ice discharge did not reduce the spread in future projections of the ice dynamics contribution to sea level compared to using observation-based basal melt sensitivities.

Basal melt was computed with a linear and quadratic relation with ocean thermal forcing. The quadratic basal melt parameterisation performs better than the linear parameterisation in reproducing past ice discharge~~.~~, especially when applied to an independent region. This is a consequence of the dependency on the absolute ocean temperature in the quadratic parameterisation, which makes the temperature-melt relation weaker in colder regions and stronger in warmer regions. Observations confirm that the quadratic relation between thermal forcing and basal melt is more realistic (Jenkins et al., 2018).

~~The projected Antarctic discharge shows a clear sensitivity to the emission scenario. Limiting emissions to scenario SSP1-2.6 compared to SSP5-8.5, would lead to about 30% reduction in the median projected sea level contribution of Antarctic discharge in 2100. The delayed feedback of ice discharge to increasing ocean temperatures (as modelled by the linear response functions) implies that the associated sea level contribution only becomes scenario-dependent after around 2050.~~

~~For the full model suite, the basal melt computation method has a greater impact on the projected~~ We find that the depth of thermal forcing has a large influence on the resulting sea level contribution ~~than the emission scenario. Across all scenarios, the median Antarctic ice loss is two times higher for the highest method than for the lowest method. Bounded calibration leads to higher median projections than unbounded calibration since all γ values are greater than zero due to the lower bound. Calibrating on the summed Antarctic response leads to higher projections than calibration per region. This can be explained by regions with a small or negative past contribution to sea level that have calibrated regional γ values equal to zero (Ross, Weddell), and therefore have no contribution in future projections even if the subsurface ocean is warming. Adapting Antarctic-wide γ values results in a positive value and positive future contribution for these regions. The basal melt parameterisation (quadratic or linear) is least important for the projections.~~ in future projections. In our study we applied the same thermal forcing depth as in Levermann et al. (2020), which is the forcing near the ice shelf base. Using a thermal forcing depth near the ice shelf base rather than the deepest ocean layer above the continental shelf leads to a larger relative contribution of the Amundsen region to the total Antarctic sea level contribution, which is closer to observations.

~~The top 10% selection gives 20-28 mm higher median projections than the full model suite. This difference can be partly attributed to~~ A drawback of the Amundsen calibration is that it overestimates the total Antarctic dynamics contribution to sea level over the historical period. However, we find a large uncertainty that is associated with intermodel spread of ESMs and RFs. Therefore, an ESM-RF pair selection is applied in which the ~~unbounded basal melt computation methods, which include γ values equal to zero for the full model suite. After selection, the top 10% γ values are greater than zero for the dominant contributing regions (Amundsen , EAIS), resulting in higher estimates. For the bounded methods, there is no significant difference between the full model selection and top 10%~~ model pairs with the best fit for the Amundsen region are selected, which are models with a higher sea level contribution in the Amundsen region. Surprisingly, the Antarctic contribution for this model selection is lower, bringing the results closer to observations.

~~This study shows that calibration of the basal melt parameterisation on past ice discharge provides a way to constrain historical and future evolution of Antarctic basal melt to observations. This leads to reduced~~ The results also show that a large part of the calibrated basal melt sensitivities are higher than those derived from melt observations, which is related to a wider spread in the ~~projections~~ calibrated basal melt sensitivities. However, even with calibration on past ice discharge, the acceleration of the sea level contribution ~~of Antarctica's ice discharge from basal melt over the 21st century. Moreover, this~~ during the observational period is underestimated, indicating missing physics.

The calibration shows that the two main studies on which the IPCC AR6 Antarctic sea level contributions are based (ISMIP6 and LARMIP-2) use median basal melt sensitivities that are higher than the median Antarctic-wide calibrated values that we found~~. If these studies would have calibrated their basal melt computations on past observations of ice discharge, this would have resulted in lower projections of Antarctica's sea level contribution.~~, but lower than the median Amundsen calibrations. The Amundsen calibration performs better in simulating the sea level acceleration and the dominance of the Amundsen region over the historical period compared to Antarctic-wide calibration, and performs arguably better than the Antarctic-wide calibration when it comes to future projections. If the Amundsen calibration would be combined with the methodological framework of

ISMIP6 and LARMIP-2 as presented in IPCC AR6, our results suggest that the estimate of the Antarctic dynamics contribution to sea level would be higher than in the original studies.

6 Code and data availability

- Linear response functions from LARMIP-2 (Levermann et al., 2020): https://github.com/ALevermann/Larmip2020/tree/master/RFunctions

- Global ocean reanalyses: https://resources.marine.copernicus.eu/product-detail/GLOBAL_REANALYSIS_PHY_001_026/INFORMATION

- Antarctic ice discharge (Rignot et al., 2019): https://www.pnas.org/doi/suppl/10.1073/pnas.1812883116/suppl_file/pnas.1812883116.sd01.xlsx

- Other code available from reasonable request to the author.

Appendix A: Hindcasts of regional sea level contributions

Figures ?? and ?? show the regional sea level contributions of the top 10% best-performing models of the quadratic parameterisation for the Antarctic-wide and regional calibration, respectively. Especially for the Weddell region, the quadratic parameterisation can be better calibrated on the observations (50% positive γ values) than the linear parameterisation (16%). This is due to the parabolic shape of the observed ice discharge over the observational period (Fig. ??). For the Weddell region, the cumulative ice discharge is close to zero, resulting in the relatively small calibrated γ values. For the Ross region, the Rignot ice discharge even shows a declining sea level contribution over the reanalysis period, which could not even be reproduced by the best fitting CMIP6 models (Fig. ??). Figure 3 consistently shows no decline in the median ocean temperature of the CMIP6 models over the historical period, pointing at a deficiency in ocean forcing for the Ross region. In the Ross region negative γ values would give a better fit for many ESM-RF pairs, but this would be physically incorrect since this would suggest that warmer temperatures lead to less basal melt and vice versa. As a consequence, a high percentage of the ESM-RF pairs has a γ with a value of zero in the Ross region. For the Peninsula, about half of the models has a γ value of zero. Consistently, most CMIP6 models do not simulate a positive temperature trend in this region over the historical period (Fig. 3), also pointing at a deficiency in the ocean forcing. For the Amundsen and EAIS regions, most models have positive calibrated γ values, consistent with the positive sea level contribution in these regions and simulated ocean warming trend over the historical period.

Regional hindcasts of the top 10% ESM-RF pairs for the QUA method over the period 1979-2017 (Table ??). The historical experiment is extended with SSP2-4.5 scenario for the years 2015-2017. The figure shows the results for the top 10% ESM-RF pairs (green), together with the Rignot ice discharge (grey). The shaded area indicates one standard deviation, representing intermodel spread for the modelled response and observational error for the Rignot data.

Same as Fig. ??, but for the QUR method.
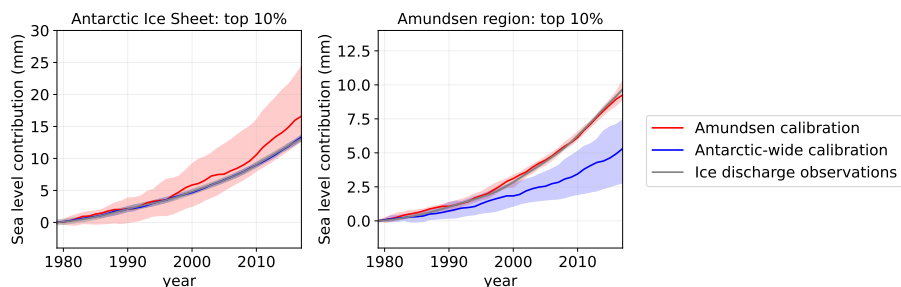
Figure A1. Similar as Fig. 6, but for top 10% best-performing ESM-RF pairs.
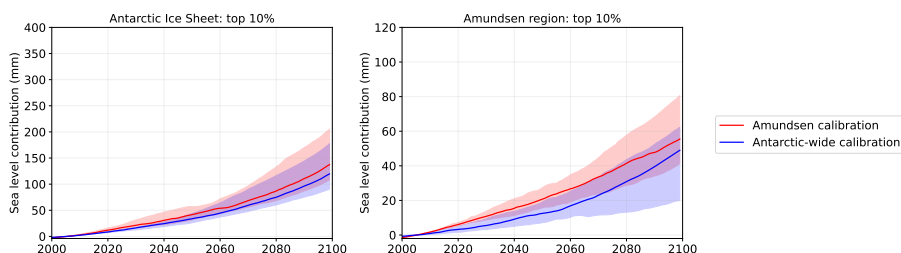
Figure A2. Similar as Fig. 7, but for top 10% best-performing ESM-RF pairs.

895 ~~Top 10% model pairs of the quadratic parameterisation with Antarctic-wide calibration (QUA). Earth system model Ice sheet modelINM-CM5-0 MALI LAN INM-CM4-8 MALI LAN EC-Earth3 ISSM JPL CAMS-CSM1-0 SICO UHO MIROC6 UA UNN INM-CM4-8 UA UNN MIROC6 ISSM UCI EC-Earth3 IMAU VUB INM-CM4-8 AISM VUB MRI-ESM2-0 CISM NCA CAMS-CSM1-0 MALI LAN MIROC6 AISM VUB MIROC6 CISM NCA MRI-ESM2-0 MALI LAN INM-CM5-0 ISSM JPL ACCESS-CM2 AISM VUB CAMS-CSM1-0 CISM NCA MRI-ESM2-0 BISI LBL 1KM CanESM5 CISM NCA~~
900 ~~MRI-ESM2-0 SICO UHO MRI-ESM2-0 ISSM JPL CAMS-CSM1-0 UA UNN~~

Author contributions. EvdL, SD and DLB designed the study. DLB downloaded the CMIP6 data from the ESGF node and wrote the code to read it. EvdL performed the computations and prepared the manuscript with contributions from all co-authors.

Competing interests. The authors declare that they have no conflict of interest.

Acknowledgements. We acknowledge the editor and two anonymous reviewers for their constructive comments which improved the quality
905 of the paper. This publication was supported by the Knowledge Programme Sea Level Rise which received funding from the Dutch Ministry
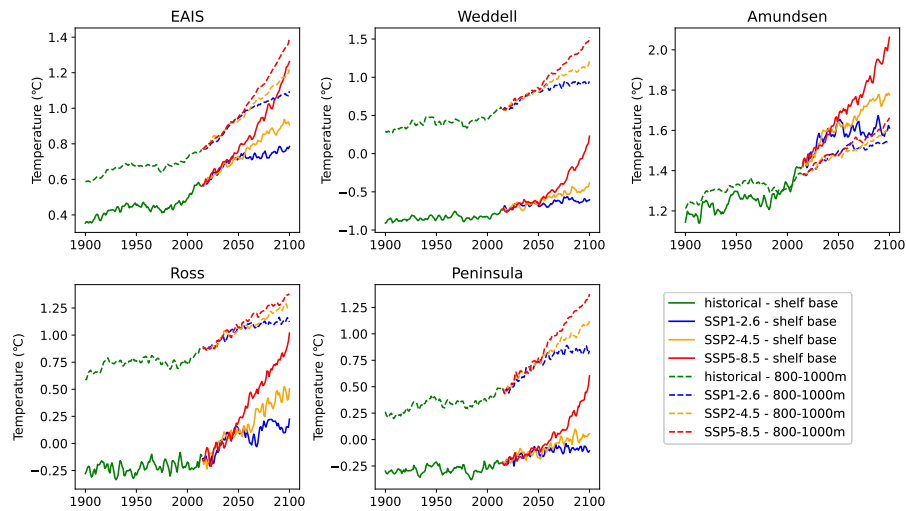
Figure A3. Annual mean subsurface ocean temperature time series of the CMIP6 multi-model mean, model drift- and bias-adjusted, for temperatures centered around the mean depth of the ice shelf base (solid lines) and temperatures between 800-1000 m depth (dashed lines).

of Infrastructure and Water Management. This publication was supported by the project RECEIPT (REmote Climate Effects and their Impact on European sustainability, Policy and Trade) which received funding from the European Union's Horizon 2020 Research and Innovation Programme under Grant agreement no. 820712. This publication was supported by PROTECT. This project has received funding from the European Union's Horizon 2020 research and innovation program under Grant agreement no. 869304, PROTECT contribution number 30.

References

Bamber, J. L. and Aspinall, W. P.: An expert judgement assessment of future sea level rise from the ice sheets, Nature Climate Change, 3, 424–427, https://doi.org/10.1038/nclimate1778, 2013.

Bamber, J. L., Oppenheimer, M., Kopp, R. E., Aspinall, W. P., and Cooke, R. M.: Ice sheet contributions to future sea-level rise from structured expert judgment, Proceedings of the National Academy of Sciences of the United States of America, 166, 11 195–11 200, https://doi.org/10.1073/pnas.1817205116, 2019.

Barthel, A., Agosta, C., Little, C. M., Hattermann, T., Jourdain, N. N., Goelzer, H., Nowicki, S., Seroussi, H., Straneo, F., and Bracegirdle, T. T.: CMIP5 model selection for ISMIP6 ice sheet model forcing: Greenland and Antarctica, Cryosphere, 14, 855–879, https://doi.org/10.5194/tc-14-855-2020, 2020.

Bronselaer, B., Winton, M., Griffies, S. M., Hurlin, W. J., Rodgers, K. B., Sergienko, O. V., Stouffer, R. J., and Russell, J. L.: Change in future climate due to Antarctic meltwater, Nature, 564, 53–58, https://doi.org/10.1038/s41586-018-0712-z, 2018.

Clark, P. U., Shakun, J. D., Marcott, S. A., Mix, A. C., Eby, M., Kulp, S., Levermann, A., Milne, G. A., Pfister, P. L., Santer, B. D., Schrag, D. P., Solomon, S., Stocker, T. F., Strauss, B. H., Weaver, A. J., Winkelmann, R., Archer, D., Bard, E., Goldner, A., Lambeck, K., Pierrehumbert, R. T., and Plattner, G. K.: Consequences of twenty-first-century policy for multi-millennial climate and sea-level change, Nature Climate Change, 6, 360–369, https://doi.org/10.1038/nclimate2923, 2016.

Dangendorf, S., Hay, C., Calafat, F. M., Marcos, M., Piecuch, C. G., Berk, K., and Jensen, J.: Persistent acceleration in global sea-level rise since the 1960s, Nature Climate Change, 9, 705–710, https://doi.org/10.1038/s41558-019-0531-8, http://dx.doi.org/10.1038/s41558-019-0531-8http://www.nature.com/articles/s41558-019-0531-8, 2019.

DeConto, R. M. and Pollard, D.: Contribution of Antarctica to past and future sea-level rise, Nature, 531, 591–597, https://doi.org/10.1038/nature17145, http://dx.doi.org/10.1038/nature17145, 2016.

Dinniman, M. S., Asay-Davis, X. S., Galton-Fenzi, B. K., Holland, P. R., Jenkins, A., and Timmermann, R.: Modeling ice shelf/ocean interaction in Antarctica: A review, Oceanography, 29, 144–153, https://doi.org/10.5670/oceanog.2016.106, 2016.

Edwards, T. L., Nowicki, S., Marzeion, B., Hock, R., Goelzer, H., Seroussi, H., Jourdain, N. C., Slater, D. A., Turner, F. E., Smith, C. J., McKenna, C. M., Simon, E., Abe-Ouchi, A., Gregory, J. M., Larour, E., Lipscomb, W. H., Payne, A. J., Shepherd, A., Agosta, C., Alexander, P., Albrecht, T., Anderson, B., Asay-Davis, X., Aschwanden, A., Barthel, A., Bliss, A., Calov, R., Chambers, C., Champollion, N., Choi, Y., Cullather, R., Cuzzone, J., Dumas, C., Felikson, D., Fettweis, X., Fujita, K., Galton-Fenzi, B. K., Gladstone, R., Golledge, N. R., Greve, R., Hattermann, T., Hoffman, M. J., Humbert, A., Huss, M., Huybrechts, P., Immerzeel, W., Kleiner, T., Kraaijenbrink, P., Le clec'h, S., Lee, V., Leguy, G. R., Little, C. M., Lowry, D. P., Malles, J. H., Martin, D. F., Maussion, F., Morlighem, M., O'Neill, J. F., Nias, I., Pattyn, F., Pelle, T., Price, S. F., Quiquet, A., Radić, V., Reese, R., Rounce, D. R., Rückamp, M., Sakai, A., Shafer, C., Schlegel, N. J., Shannon, S., Smith, R. S., Straneo, F., Sun, S., Tarasov, L., Trusel, L. D., Van Breedam, J., van de Wal, R., van den Broeke, M., Winkelmann, R., Zekollari, H., Zhao, C., Zhang, T., and Zwinger, T.: Projected land ice contributions to twenty-first-century sea level rise, Nature, 593, 74–82, https://doi.org/10.1038/s41586-021-03302-y, 2021.

Eyring, V., Bony, S., Meehl, G. A., Senior, C. A., Stevens, B., Stouffer, R. J., and Taylor, K. E.: Overview of the Coupled Model Intercomparison Project Phase 6 (CMIP6) experimental design and organization, Geoscientific Model Development, 9, 1937–1958, https://doi.org/10.5194/gmd-9-1937-2016, 2016.

945 Favier, L., Jourdain, N. C., Jenkins, A., Merino, N., Durand, G., Gagliardini, O., Gillet-Chaulet, F., and Mathiot, P.: Assessment of Sub-Shelf Melting Parameterisations Using theOcean-Ice Sheet Coupled Model NEMO(v3.6)-Elmer/Ice(v8.3), Geoscientific Model Development Discussions, pp. 1–40, https://doi.org/10.5194/gmd-2019-26, 2019.

Fox-Kemper, B., H. T. Hewitt, C. Xiao, G. Aðalgeirsdóttir, S. S. Drijfhout, T. L. Edwards, N. R. Golledge, M. Hemer, R. E. Kopp, G. Krinner, A. Mix, D. Notz, S. Nowicki, I. S. Nurhati, L. Ruiz, Sallée, J.-B., Slangen, A. B. A., and Yu, Y.: Ocean, Cryosphere and Sea Level Change,
950 Tech. rep., 2021.

Golledge, N. R., Keller, E. D., Gomez, N., Naughten, K. A., Bernales, J., Trusel, L. D., and Edwards, T. L.: Global environmental conse- quences of twenty-first-century ice-sheet melt, Nature, 566, 65–72, https://doi.org/10.1038/s41586-019-0889-9, http://dx.doi.org/10.1038/ s41586-019-0889-9, 2019.

Haasnoot, M., Kwadijk, J., Van Alphen, J., Le Bars, D., Van Den Hurk, B., Diermanse, F., Van Der Spek, A., Oude Essink, G., Delsman, J.,
955 and Mens, M.: Adaptation to uncertain sea-level rise; how uncertainty in Antarctic mass-loss impacts the coastal adaptation strategy of the Netherlands, Environmental Research Letters, 15, https://doi.org/10.1088/1748-9326/ab666c, 2020.

Hinkel, J., Lincke, D., Vafeidis, A. T., Perrette, M., Nicholls, R. J., Tol, R. S., Marzeion, B., Fettweis, X., Ionescu, C., and Levermann, A.: Coastal flood damage and adaptation costs under 21st century sea-level rise, Proceedings of the National Academy of Sciences of the United States of America, 111, 3292–3297, https://doi.org/10.1073/pnas.1222469111, 2014.

960 Hinkel, J., Feyen, L., Hemer, M., Cozannet, G., Lincke, D., Marcos, M., Mentaschi, L., Merkens, J. L., Moel, H., Muis, S., Nicholls, R. J., Vafeidis, A. T., Wal, R. S. W., Vousdoukas, M. I., Wahl, T., Ward, P. J., and Wolff, C.: Uncertainty and Bias in Global to Regional Scale Assessments of Current and Future Coastal Flood Risk, Earth's Future, 9, https://doi.org/10.1029/2020ef001882, 2021.

Jenkins, A., Shoosmith, D., Dutrieux, P., Jacobs, S., Kim, T. W., Lee, S. H., Ha, H. K., and Stammerjohn, S.: West Antarctic Ice Sheet retreat in the Amundsen Sea driven by decadal oceanic variability, Nature Geoscience, 11, 733–738, https://doi.org/10.1038/s41561-018-0207-4,
965 http://dx.doi.org/10.1038/s41561-018-0207-4, 2018.

Jourdain, N. C., Asay-Davis, X., Hattermann, T., Straneo, F., Seroussi, H., Little, C. M., and Nowicki, S.: A protocol for calculating basal melt rates in the ISMIP6 Antarctic ice sheet projections, The Cryosphere, 14, 3111–3134, https://doi.org/10.5194/tc-14-3111-2020, https: //tc.copernicus.org/articles/14/3111/2020/, 2020.

Lambert, E., Le Bars, D., Goelzer, H., and van de Wal, R. S.: Correlations Between Sea-Level Components Are Driven by Regional Climate
970 Change, Earth's Future, 9, 1–17, https://doi.org/10.1029/2020EF001825, 2021.

Levermann, A., Winkelmann, R., Nowicki, S., Fastook, J. L., Frieler, K., Greve, R., Hellmer, H. H., Martin, M. A., Meinshausen, M., Mengel, M., Payne, A. J., Pollard, D., Sato, T., Timmermann, R., Wang, W. L., and Bindschadler, R. A.: Projecting Antarctic ice discharge using response functions from SeaRISE ice-sheet models, Earth System Dynamics, 5, 271–293, https://doi.org/10.5194/esd-5-271-2014, 2014.

Levermann, A., Winkelmann, R., Albrecht, T., Goelzer, H., Golledge, N. R., Greve, R., Huybrechts, P., Jordan, J., Leguy, G., Martin, D.,
975 Morlighem, M., Pattyn, F., Pollard, D., Quiquet, A., Rodehacke, C., Seroussi, H., Sutter, J., Zhang, T., Van Breedam, J., Calov, R., Deconto, R., Dumas, C., Garbe, J., Hilmar Gudmundsson, G., Hoffman, M. J., Humbert, A., Kleiner, T., Lipscomb, W. H., Meinshausen, M., Ng, E., Nowicki, S. M., Perego, M., Price, S. F., Saito, F., Schlegel, N. J., Sun, S., and Van De Wal, R. S.: Projecting Antarctica's contribution to future sea level rise from basal ice shelf melt using linear response functions of 16 ice sheet models (LARMIP-2), Earth System Dynamics, 11, 35–76, https://doi.org/10.5194/esd-11-35-2020, 2020.

980 Little, C. M. and Urban, N. M.: CMIP5 temperature biases and 21st century warming around the Antarctic coast, Annals of Glaciology, 57, 69–78, https://doi.org/10.1017/aog.2016.25, 2016.

Liu, Y., Moore, J. C., Cheng, X., Gladstone, R. M., Bassis, J. N., Liu, H., Wen, J., and Hui, F.: Ocean-driven thinning enhances iceberg calving and retreat of Antarctic ice shelves, Proceedings of the National Academy of Sciences of the United States of America, 112, 3263–3268, https://doi.org/10.1073/pnas.1415137112, 2015.

985 Mathiot, P., Jenkins, A., Harris, C., and Madec, G.: Explicit representation and parametrised impacts of under ice shelf seas in the z_*-coordinate ocean model NEMO 3.6, Geoscientific Model Development, 10, 2849–2874, https://doi.org/10.5194/gmd-10-2849-2017, 2017.

Nerem, R. S., Beckley, B. D., Fasullo, J. T., Hamlington, B. D., Masters, D., and Mitchum, G. T.: Climate-change–driven accelerated sea-level rise detected in the altimeter era, Proceedings of the National Academy of Sciences of the United States of America, 115, 2022–2025, https://doi.org/10.1073/pnas.1717312115, 2018.

990 Nowicki, S., Goelzer, H., Seroussi, H., Payne, A. J., Lipscomb, W. H., Abe-Ouchi, A., Agosta, C., Alexander, P., Asay-Davis, X. S., Barthel, A., Bracegirdle, T. J., Cullather, R., Felikson, D., Fettweis, X., Gregory, J. M., Hattermann, T., Jourdain, N. C., Kuipers Munneke, P., Larour, E., Little, C. M., Morlighem, M., Nias, I., Shepherd, A., Simon, E., Slater, D., Smith, R. S., Straneo, F., Trusel, L. D., Van Den Broeke, M. R., and Van De Wal, R.: Experimental protocol for sea level projections from ISMIP6 stand-alone ice sheet models, Cryosphere, 14, 2331–2368, https://doi.org/10.5194/tc-14-2331-2020, 2020.

995 Nowicki, S. M., Payne, A., Larour, E., Seroussi, H., Goelzer, H., Lipscomb, W., Gregory, J., Abe-Ouchi, A., and Shepherd, A.: Ice Sheet Model Intercomparison Project (ISMIP6) contribution to CMIP6, Geoscientific Model Development, 9, 4521–4545, https://doi.org/10.5194/gmd-9-4521-2016, 2016.

Palmer, M. D., Gregory, J. M., Bagge, M., Calvert, D., Hagedoorn, J. M., Howard, T., Klemann, V., Lowe, J. A., Roberts, C. D., Slangen, A. B., and Spada, G.: Exploring the Drivers of Global and Local Sea-Level Change Over the 21st Century and Beyond, Earth's Future, 8,
1000   https://doi.org/10.1029/2019EF001413, 2020.

Pritchard, H. D., Ligtenberg, S. R., Fricker, H. A., Vaughan, D. G., Van Den Broeke, M. R., and Padman, L.: Antarctic ice-sheet loss driven by basal melting of ice shelves, Nature, 484, 502–505, https://doi.org/10.1038/nature10968, 2012.

Rignot, E. and Jacobs, S. S.: Rapid bottom melting widespread near antarctic ice sheet grounding lines, Science, 296, 2020–2023, https://doi.org/10.1126/science.1070942, 2002.

1005 Rignot, E., Mouginot, J., Scheuchl, B., Van Den Broeke, M., Van Wessem, M. J., and Morlighem, M.: Four decades of Antarctic ice sheet mass balance from 1979–2017, Proceedings of the National Academy of Sciences of the United States of America, 116, 1095–1103, https://doi.org/10.1073/pnas.1812883116, 2019.

Sadai, S., Condron, A., DeConto, R., and Pollard, D.: Future climate response to Antarctic Ice Sheet melt caused by anthropogenic warming, Science Advances, 6, 1–9, https://doi.org/10.1126/sciadv.aaz1169, 2020.

1010 Seroussi, H., Nowicki, S., Payne, A. J., Goelzer, H., Lipscomb, W. H., Abe-Ouchi, A., Agosta, C., Albrecht, T., Asay-Davis, X., Barthel, A., Calov, R., Cullather, R., Dumas, C., Galton-Fenzi, B. K., Gladstone, R., Golledge, N. R., Gregory, J. M., Greve, R., Hattermann, T., Hoffman, M. J., Humbert, A., Huybrechts, P., Jourdain, N. C., Kleiner, T., Larour, E., Leguy, G. R., Lowry, D. P., Little, C. M., Morlighem, M., Pattyn, F., Pelle, T., Price, S. F., Quiquet, A., Reese, R., Schlegel, N. J., Shepherd, A., Simon, E., Smith, R. S., Straneo, F., Sun, S., Trusel, L. D., Breedam, J. V., Van De Wal, R. S., Winkelmann, R., Zhao, C., Zhang, T., and Zwinger, T.: ISMIP6 Antarctica: A multi-model
1015   ensemble of the Antarctic ice sheet evolution over the 21st century, Cryosphere, 14, 3033–3070, https://doi.org/10.5194/tc-14-3033-2020, 2020.

Shepherd, A., Ivins, E., Rignot, E., Smith, B., van den Broeke, M., Velicogna, I., Whitehouse, P., Briggs, K., Joughin, I., Krinner, G., Nowicki, S., Payne, T., Scambos, T., Schlegel, N., A, G., Agosta, C., Ahlstrøm, A., Babonis, G., Barletta, V., Blazquez, A., Bonin, J., Csatho, B., Cullather, R., Felikson, D., Fettweis, X., Forsberg, R., Gallee, H., Gardner, A., Gilbert, L., Groh, A., Gunter, B., Hanna, E., Harig, C.,

1020   Helm, V., Horvath, A., Horwath, M., Khan, S., Kjeldsen, K. K., Konrad, H., Langen, P., Lecavalier, B., Loomis, B., Luthcke, S., McMillan, M., Melini, D., Mernild, S., Mohajerani, Y., Moore, P., Mouginot, J., Moyano, G., Muir, A., Nagler, T., Nield, G., Nilsson, J., Noel, B., Otosaka, I., Pattle, M. E., Peltier, W. R., Pie, N., Rietbroek, R., Rott, H., Louise Sandberg-Sørensen, Ingo Sasgen, H. S., Scheuchl, B., Schrama, E., Schröder, L., Seo, K.-W., Simonsen, S., Slater, T., Spada, G., Sutterley, T., Talpe, M., Tarasov, L., van de Berg, W. J., van der Wal, W., van Wessem, M., Vishwakarma, B. D., Wiese, D., and Wouters, B.: Mass balance of the Antarctic Ice Sheet from 1992 to 2017,
1025   Nature, 558, 219–222, https://doi.org/10.1038/s41586-018-0179-y, http://www.nature.com/articles/s41586-018-0179-y, 2018.

Thompson, A. F., Stewart, A. L., Spence, P., and Heywood, K. J.: The Antarctic Slope Current in a Changing Climate, Reviews of Geophysics, 56, 741–770, https://doi.org/10.1029/2018RG000624, 2018.

van de Wal, R. S., Zhang, X., Minobe, S., Jevrejeva, S., Riva, R. E., Little, C., Richter, K., and Palmer, M. D.: Uncertainties in Long-Term Twenty-First Century Process-Based Coastal Sea-Level Projections, Surveys in Geophysics, 40, 1655–1671,
1030   https://doi.org/10.1007/s10712-019-09575-3, https://doi.org/10.1007/s10712-019-09575-3, 2019.

van den Broeke, M.: Strong surface melting preceded collapse of Antarctic Peninsula ice shelf, Geophysical Research Letters, 32, 1–4, https://doi.org/10.1029/2005GL023247, 2005.